UNDERSTANDING THE COMPLEX INTERPLAY BETWEEN *MYCOBACTERIUM AVIUM* SUBSPECIES *PARATUBERCULOSIS* AND THE BOVINE MACROPHAGE

By

Edward Alan Kabara

A DISSERTATION

Submitted to
Michigan State University
in partial fulfillment of the requirements
for the degree of

DOCTOR OF PHILOSPHY

Natural Science

2011

ABSTRACT

UNDERSTANDING THE COMPLEX INTERACTION BETWEEN *MYCOBACTERIUM AVIUM* SUBSPECIES *PARATUBERCULOSIS* AND THE BOVINE MACROPHAGE

By

Edward Alan Kabara

Mycobacterium avium subspecies *paratuberculosis* (MAP) is a significant concern both to the American Dairy industry and in regards to human health. MAP causes a chronic inflammatory disease in ruminants known as Johne's disease. Johne's disease affects over 68% of American dairy farms and causes over $1.5 billion in losses each year to the dairy industry. Pasteurization does not destroy all MAP bacteria. Therefore, viable MAP has been detected in commercially available milk, meat, and cheese. Further troubling, MAP has been linked to the human inflammatory condition known as Crohn's disease. The root cause of the chronic inflammation in these diseases is the ability of MAP to prevent macrophage phagosome maturation and intracellular survival. Our group, the molecular pathogenesis laboratory, is interested in the complex interactions between the infecting MAP bacteria and the host macrophage. Previously, we found that MAP altered the transcriptome of infected cultures. Based on these results, my work focused on studying the common pathways altered in MAP-infected macrophages. My initial work used 10 different MAP strains isolated from four different species. By using such a large variety of MAP strains, we established the transcriptome elements that are commonly altered in MAP infection. Through this work, we found several host pathways that are altered in MAP infection. As part of this work, we reannotated the BOTL5 microarray. To help other researchers, we provided the methodology and scripts necessary for easy reannotation of other

microarrays. Among the pathways altered in MAP-infected macrophages, we found apoptosis to be regulated. Continuing our studies in this area, we found significant differences between MAP-infected macrophages and uninfected culture mates. Our studies also indicated that regulation of caspase activation and transcription may explain the different levels of apoptosis in MAP-infected and control cells. The net result of our work was a deeper understanding of the complex interaction between the bovine macrophages and infecting MAP with a particular focus on MAP-mediated regulation of host cell apoptosis.

DEDICATION

To my Dad, Mom, brothers, sister, and my wife. Thanks for believing in me.

ACKNOWLEDGEMENTS

I would like to thank my committee members, Dr. Feig, Dr. DellaPenna, Dr. Chan, Dr. Knott, and Dr. Punch for their support and guidance through this project.

I would like to thank Dr. Coussens for his mentorship through my entire graduate career. I would also like to thank Sue Sipkowsky and Chris Colvin for helping make this project successful. I also must thank my friends Dr. Mindy Wilson and Amber Wilson for a thorough review of my writing.

TABLE OF CONTENTS

LIST OF TABLES

LIST OF FIGURES

Chapter 1

Introduction

Johne's disease is a worldwide problem affecting both agriculturally important animals such as dairy cattle and wildlife such as deer. This disease, caused by the bacterium *Mycobacterium avium* subspecies *paratuberculosis* (MAP), leads to chronic bowl inflammation. Since no effective vaccine or treatment is currently available, spread of the disease remains unchecked. Even more of a concern is the link between Johne's disease in animals and Crohn's disease in humans[1].

Johne's disease presents a serious concern to the world-wide food supply. In the American dairy industry alone, Johne's disease accounts for over $1.5 billion in losses each year due to decreased milk production, reduced weight at time of sale, treatment costs, and replacement stock[2]. More troubling, over 68% of cattle herds in the dairy industry are infected[1]. Major methods of detection (PCR based fecal analysis, ELISA, and fecal bacteria culture) have a high degree of false negative results and rarely agree with one another. Therefore, an animal's actual Johne's disease status is uncertain [3]. The actual number of infected animals on a particular farm may be much higher than the currently accepted number due to discrepancies between testing methods. Therefore, culling and replacing animals with uninfected stock is an inefficient way to eradicate the disease. Replacement animals may unintentionally introduce new strains or additional bacterium into the environment. Samples of animal feed grass taken from infected farms, that use MAP-contaminated manure as a fertilizer, have been found to contain viable bacteria as long as one year post-contamination. This demonstrates that MAP persists in the environment for extended periods of time [4]. These

studies indicate that MAP is a devastating infectious agent in the American food industry with several complicating factors and few available methods to significantly control Johne's disease.

MAP affects not only the food industry, but the health of the human population. It is known as the cause of Johne's disease and has been implicated as the causative agent of a similar chronic inflammatory disease in humans, Crohn's disease. Studies on the connection between these two disease dates as far back as 1913[5]. Both Johne's and Crohn's are know for a long latency period followed by severe intestinal inflammation and wasting of the infected individual[5]. In addition, more and more data indicates that MAP is also the causative agent of Crohn's disease as MAP is often detected in infected individuals[5]. If MAP causes both of these gastroenteric diseases, then the high prevalence and persistence of MAP bacteria in the dairy and meat industry is alarming. In addition to the dairy industry factors regarding the prevalence of MAP, pasteurization, the main method used to sterilize dairy products, is not 100% effective against MAP. Both the high temperature/quick exposure and low temperature/long exposure methods used to sterilize milk before distribution fail to completely eradicate the bacterium from products that are available to the general public [6]. MAP has been isolated from commercially available milk, meat, and cheese samples. Therefore, the general public is at risk of being exposed to an active infectious agent through dairy products [6]. Thus, studying the progression and survival of MAP is an extremely important research goal if we wish to protect the USA's food supply.

MAP generally infects the host at an exceptionally early age. Calves are often exposed as soon as they take infected milk from a MAP-positive dam [7]. However, even if the calf is prevented from receiving milk from an infected mother, feces is another route of exposure as calves come into contact with MAP via the oral-fecal route [7]. Following bacterial exposure,

the bacteria enters host macrophages via microfold-cells in the intestine. MAP is transported to intestinal macrophages and is phagocytized by these macrophages. At this point the normal phagosome maturation pathway is interrupted, and MAP is able to survive for long periods of time inside host macrophages. Macrophages with stalled phagosomes then become a reservoir for the bacteria leading to a chronic infection in the host [7]. Initially in MAP infection, the host responds in a cell-mediated inflammatory response. This response allows for control of the bacteria and causes macrophages to phagocytize and destroy MAP bacteria [8]. However, over time the host's immune response switches from the cell-mediated response to an antibody-mediated response. Because antibodies are unable to enter infected macrophages, the antibody mediated-response is far less able to control the bacteria. Furthermore, as part of the antibody-mediated response the host down-regulates the cell-mediated response, which means that even fewer cells are able to properly destroy the bacteria. The end result of this switch in immune response is a better environment for the bacteria to survive inside of the host macrophage[8]. Moreover, as the amount of intracellular MAP bacteria increases, more inflammatory damage is done to the host. Increased inflammatory damage to the host intestines, possibly mediated by IL-1 , causes the wasting, diarrhea, and eventual death that are indicative of Johne's disease [8, 9]. MAP bacteria spread via feces. As the bacterial load in the infected animal increases, more bacteria are then shed into the feces of the infected animal. This causes other animals to become infected as they share living space with MAP-positive animals [7].

One of the most notable aspects of MAP infection is the intracellular survival of the bacteria in macrophages. MAP is taken up by macrophages using many receptors such as CD14 and the mannose receptor. However, no one specific receptor utilized can effectively initiate complete neutralization of the bacteria[10]. After uptake of the bacteria, the phagosome

containing the bacteria undergoes some maturation as other cell vacuoles merge momentarily with the phagosome adding markers, proteins, and chemicals such as reactive nitrogen and oxygen species[11]. Over the course of maturation, phagosomes receive the RAB5 marker and become acidified to a pH of approximately 6.25[12]. However, the phagosome fails to become acidic enough to destroy the bacteria and never receives the LAMP marker from fusion with lysosomes, indicating a failure to progress through the endocytic pathway [12]. Proteins in the phagolysosome maturation and degradation pathway fail to enter the MAP-containing vacuole [12] thus the bacteria can survive and replicate in the cell. While several theories exist, it is unknown exactly how MAP-infection of the macrophage prevents phagosome maturation. It is known however, that intracellular survival of MAP and macrophage phagosome maturation prevents proper immune signaling [8]. The survival of infected macrophages allows the bacteria to not only survive, but masks its presence from the host at large.

Our particular interest in Johne's disease focuses on this last area of MAP-macrophage interaction. While several groups have studied this interaction, none have led to development of comprehensive theories that would explain the mechanisms for intracellular survival of the bacteria. Our goal is to better understand how MAP can survive within macrophage cells. Through a better understanding of this host-pathogen relationship, we hope to develop treatments and vaccines for both Johne's and Crohn's disease.

For my work, I began studying the host-pathogen interaction via a large-scale microarray project studying the expression of over 1300 host genes in experimental infection of macrophage cells from five different cows. Through this initial screening, we found several host genes that were differentially regulated in MAP infection and several host pathways that may play a significant role in MAP intracellular survival in macrophages. In addition, I reannotated the

microarray and contributed a significant number of annotations to the known proteins whose genes were represented on the array. We made the annotation method and scripts publicly available (manuscript in preparation, chapter 3). One of the major pathways implicated by the microarray work involved programmed cell death or apoptosis. Through careful study of cultured primary bovine macrophages, we found significant differences between the apoptotic profiles of cells infected with MAP, uninfected culture mates, and cells from uninfected control cultures. Based on this, I studied specific bovine proteins that may be involved in the regulation of host cell apoptosis and prevention of immune signaling.

The first step in the study of specific genes was the microarray project. This microarray project was one of the largest dual color microarray experiments conducted; we compared 10 different strains of MAP bacteria and determined how MAP-infection modified the transcriptome profile of macrophages prepared from five different healthy Holstein cattle. We found that over 90 transcripts on the BOTL5 microarray are differentially regulated in MAP-infected macrophage cultures. Additionally, we found that over 60 of these spots could be annotated and compared to human sequences. This lead to a better understanding of the role these genes may play in MAP infection. Using the human annotations, I studied the known annotations of these sequences and found several host pathways that are important in MAP-infected macrophages. I also studied the transcriptome profile of macrophages infected by 10 different MAP strains. Of these 10 strains, I found that a commonly used laboratory strain, K10, altered the host macrophage transcriptome differently than the other strains. Thus, K10 was a clear outlier when compared to the other strains. Through the microarray project, we found that apoptosis is a predominant host pathway found to be altered in MAP-infections. Interestingly, we discovered that experiments studying whole cell cultures may be complicated by intra-culture

cell differences. Specifically, we found that a phenomenon called the "bystander effect" could cause complications in the interpretation of whole culture data. The bystander effect causes uninfected cells within an infected culture, to show significant differences from the infected cells. Since "whole culture" data reflects an *average* response, differences among cells in a culture can contradict one another, masking subtle differences occurring within the culture. To better study this phenomenon, we used flow cytometry to study MAP-infected and uninfected macrophages within the same culture. Using this method, we found that populations of bystander, MAP-infected, and control cells from uninfected cultures differ significantly from one another in terms of apoptosis and that MAP-infected macrophage populations have a much lower percentage of apoptotic macrophages than the other two cell populations. In addition, we studied how MAP-infection alters the regulation of apoptosis. Data indicated that host cell caspase activation and expression are significantly different in infected macrophages than control cultures, leading us to believe that this may be a mechanism of bacterial control of host apoptosis. Furthermore, we also studied host cell expression of several proteins involved in apoptosis and found significant differences from control cells suggesting a mechanism for MAP-driven control of host cell death.

Chapter 2

A Large-Scale Study of Differential Gene Expression in Monocyte-Derived Macrophages Infected with several strains of *Mycobacterium avium* subspecies *paratuberculosis*

E. Kabara[1], C.C. Kloss[2], M. Wilson[3], S. Sreevatsan[4], H. Janagama[4], and P.M. Coussens[2].

[1]Department of Biochemistry and [2]Center for Animal Functional Genomics, Department of Animal Science, Michigan State University, East Lansing, MI. [3]Science Department, Lansing Community College, Lansing, MI [4]Center for Animal Health and Food Safety, University of Minnesota, Minneapolis, MN.

Abstract

Mycobacterium avium subspecies paratuberculosis (MAP) is a significant concern to the American and European dairy industries and possibly to human health. MAP possesses the rare ability to survive and replicate in infected macrophages, cells that are typically able to destroy pathogens. Little is known about what changes occur in MAP-infected macrophages that prevent phagosome maturation and lead to intracellular survival of the bacteria. In this study, a bovine immunologically specific cDNA microarray was used to study genes whose expression was altered in monocyte-derived macrophages (MDM) when these cells were infected with 10 different strains of MAP bacteria. Although we used MAP strains isolated from 4 different host species, cluster analysis of each strains influence in infected MDMs showed no species of origin

specific MAP alterations in the host transcriptome. However, MAP strain K10 was observed as a clear outlier in the cluster analysis. Additionally, we observed two SuperShedder MAP strains clustering very closely together compared to the other strains in this study. Overall, microarray analysis yielded 78 annotated genes whose expression was altered by MAP infection, regardless of strain. Few of these genes have been previously studied in the context of Johne's disease or other mycobacterium-caused diseases. Large groups of apoptosis genes, transcription factors, and cytokines were found to be differentially expressed in infected monocyte-derived macrophages as well as several genes not previously linked to MAP-host interactions. Identifying novel host genes affected by MAP infection of macrophages may lead to a more complete picture of this complex host-pathogen interaction.

Introduction

Mycobacterium avium subspecies *paratuberculosis*, the causative agent of Johne's disease in cattle, is a facultative intracellular pathogen that preferentially resides in host intestinal macrophages [13], causing granulomatous enteritis, persistent diarrhea, chronic wasting, and eventually death [14]. Johne's disease ranks as one of the most costly infectious diseases in dairy cattle resulting in a loss to the American dairy industry of over 1.5 billion dollars per year [2].

MAP transmission occurs mainly through the fecal-oral route [13] and the bacteria, which can survive for over 50 weeks in the environment, is shed in feces of infected animals [4], thereby exposing other animals within the herd. Furthermore, MAP has been shown to live in reservoirs other than mammals, such as nematodes, which could spread the pathogen to new environments [15], making control of this disease extremely difficult. Since discovery of the

bacterium in 1895, the scientific community's knowledge of MAP pathogenesis has increased steadily, but there are no cost-effective therapies for Johne's disease and vaccination, which is not currently used in the U.S., is only marginally effective [13, 16, 17].

The diagnosis of Johne's disease is based on serum or milk ELISA, production of IFN-γ by stimulated T cells, and fecal culture tests, however the sensitivity of any individual test is often low due primarily to a high rate of false negative results [18]. A long (2-5 years) subclinical phase of infection also complicates diagnosis and control measures. Thus, the global dairy industry is unable to completely prevent MAP transmission to uninfected herds or to remove MAP entirely from the food supply [18-20]. The inability to prevent contaminated milk or animal products from reaching consumers may pose some human health concerns. Recent studies have shown that MAP may be a causative or exacerbating factor in some cases of human Crohn's disease [5], a chronic inflammatory bowel disease characterized by transmural inflammation and granuloma formation [21]. The similarities between Johne's disease and Crohn's disease lead some authors to speculate that Crohn's disease is the human form of Johne's disease [13]. Widespread acceptance of this hypothesis still requires further investigation and evidence, but this association highlights the potential zoonotic nature of MAP infection.

A closely related pathogen that shares characteristics with MAP, such as survival within macrophages, is *Mycobacterium tuberculosis* (Mtb), the causative agent of tuberculosis. Much like MAP, this pathogen can prevent phagosome maturation, leading to intracellular persistence. The precise molecular mechanisms used by Mtb to persist within macrophages are, as in the case of MAP, unknown [22]. Mtb has a significant impact on human health as one-third of the world's population is infected with tuberculosis [23]. Antibiotics and radiation treatments have been used to treat Mtb infection. However, antibiotic resistant strains of Mtb have emerged and

make control of tuberculosis in the future a worldwide concern [24]. Antibiotic resistant strains of Mtb underscore the importance of developing new treatments for tuberculosis. Understanding the interplay between MAP and macrophages may also help to reveal new aspects of Mtb pathophysiology resulting in development of new therapies to control both diseases.

Despite the overwhelming importance of Johne's disease to the global dairy industry, it is clear that our knowledge of the bovine immune response to MAP (as well as other pathogens), although improving, is sparse. From work *in vivo*, it is clear that infected cattle initially develop an early and appropriate pro-inflammatory T helper type 1 (T_H1) and cytotoxic immune response to MAP antigens. However, this response typically declines during the long subclinical phase of infection, and a T_H2 response becomes predominant, but is ineffective at controlling the bacteria [25]. It is also known that MAP is able to halt normal phagosome maturation in infected cells, being able to persist and multiply within the infected host phagosome [25]. At present, it is unclear which molecular mechanisms are used by MAP to survive in macrophages, how MAP-infected macrophages persist in intestinal tissues, or how MAP-infected macrophages interact with other components of the host immune system.

Previous studies have shown that MAP alters host macrophage transcriptomes. Also, recent results have shown that there is a difference in host gene transcription between pathogenic mycobacteria and non-pathogenic bacteria [26]. In the current report, our overall hypothesis was that there exists a core group of host macrophage genes transcriptionally altered by virulent MAP infection.

To test our hypothesis, we utilized 10 strains of MAP isolated from 4 different species to infect bovine MDMs and to determine, by bovine total leukocyte microarray (BOTL5), which

host genes are induced or suppressed during MAP infection relative to uninfected macrophages. This study 1) identified genes differentially regulated early in MAP infection in bovine MDM cells and 2) observed biphasic clustering of different MAP strains based on distinct alterations of the bovine MDM transcriptome.

Methodology

Bacterial Culture. One MAP strain (ATCC #19698) was obtained from the American Type Culture Collection and the remaining strains (SS140, SS149, 1018, 7560, 7565, MAP5, MAP6, 5001, and K10) were collected as previously described[27]. The strains used were from four different species: bovine (ATCC #19698, SS149, SS140, K10, 1018), ovine (7565, 5001), bison (7560), and human (MAP5, MAP6). All strains were cultured at 37^0C in Middlebrooks 7H9 media with 10% Middlebrooks OADC and 2mg/l Mycobactin J (Allied Monitor, Lexana, KS) [26].

Animal Selection and Bovine Monocyte-Derived Macrophage Cell Culture. Blood was collected from five uninfected Holstein cows. Peripheral blood mononuclear cells (PBMC) were isolated using a Percoll gradient (1.084 g/cm^3) and seeded onto 25cm^2 flasks at 1x10^8 PBMC per flask. Non-adherent cells were removed 4 hours after plating by rinsing with Phosphate Buffered Saline (PBS). The cells were cultured for seven days to select for MDMs [9]. A more in-depth explanation of the procedure is described in Murphy et al., [26]. Unlike in Murphy et al., autologous serum from each cow was used to coat the flasks and as 10% media supplement in place of Fetal Bovine Serum (FBS) to improve yield of macrophages, improve cell quality, and ability to phagocytize cells [28]. Autologous serum was heat-inactivated at 56^{o}C for 20 minutes,

cooled for 10 minutes at room temperature, centrifuged for 20 minutes, and the supernatant was collected.

Preparation of Reference RNA. RNA from uninfected MDM cells was collected for each of the five cows using the Versagene Kit from Gentra Systems (Minneapolis, MN). These samples were used as reference RNA on the BOTL5 microarrays. By creating a pool of reference RNA that is specific for each individual cow, additional strains of bacteria could be easily added to this experiment at any time through a reference design as opposed to other microarray experiment designs. Additionally, by using a reference pool for each animal, each animals individual bias would be accounted for as the control and infected sample would come from the same animal instead of a pool of several animals [29]. Due to the need for over 110 ug of reference RNA for all 10 microarrays, it was necessary to isolate cells on several different days and to pool all the RNA together to gain a single homogeneous reference sample for each animal. Reference RNA for each animal was assayed for quality and quantity using the RNA Integrity Number (RIN, minimum of 7.5) from the Bioanalyser 2100 (Agilent Technologies, Palo Alto, CA) both before and after pooling.

Infection of Bovine MDM. After 7 days in culture, MDM cells from each cow were assigned into two groups; one group was infected with MAP using each test strain in a separate infection [26] the other group within cow served as an uninfected control. All cell cultures were infected at a multiplicity of infection of 5:1 (MAP:Cells). At 6 hours post infection, cells were harvested and RNA was extracted using the Versagene kit [26]. All RNA was tested for quality using the Agilent Bioanalyser 2100 to verify the RNA had a RNA Integrity Number (RIN) of $\geq$7.5.

cDNA synthesis and Microarray Hybridization. Using 10 μg of total RNA from each cows´ reference pool and 10 μg of total RNA from each individual MAP strain infection, cDNA was synthesized using a reverse transcription reaction (SuperScript Indirect cDNA Labeling System, Invitrogen, Carlsbad, CA). After purification of the first-strand cDNA, the reference cDNA was labeled with Cy5 dye and infected sample cDNA was labeled with Cy3 dye (CyDye post-labeling reactive labs, GE Healthcare, Piscataway, NJ). After removing un-hybridized dye, labeled samples were combined and hybridized to BOTL5 microarray as described by Murphy et al. [26].

Real time qRT-PCR Validation

To gather RNA for validation Real Time qRT-PCR, MAP infections were performed in MDM cells from six different uninfected Holstein cattle. To simplify this study, representative strains from each of two major MAP clades identified in clustering of the original microarray data were selected; this selection is discussed further in the paper. The two MAP strains selected for Real Time qRT-PCR analysis were strains 1018 and ATCC #19698 (ATCC). Real Time qRT-PCR primers and methods were derived and performed as previously described in Murphy et al. with one exception of using 30 ng of cDNA for each reaction [26]. A full list of primers and sequences are available on the Center for Animal Genomics website (http:/www.cafg.msu.edu).

Data Analysis. Microarray data was normalized using the LOESS method as previously described in Murphy et al. [26]. After normalization, the data was converted to Log10 space and the reference value was subtracted from the infected value to find the fold difference from reference for each gene. To correct for cow-specific differences in expression, a mixed-model analysis was performed, employing the SAS program essentially as described by Allison et al.

[30]. Each strain-specific dataset represents the average signal intensity for each gene over all microarrays used to examine this MAP strain. Cluster analysis was performed using the Cluster 3.0 program with averaged data from each strain [31]. Then, strain-specific data was averaged to create a composite strain. The composite strain data is thus a generated data set representing the average effect that all strains in the study had on the host transcriptome and was used to determine significantly altered genes during infection. To look for enrichment in various known aspects of each of the genes from the microarray, the Database for Annotation, Visualization and Integrated Discovery (DAVID, http://david.abcc.ncifcrf.gov/) analysis program was used as described on the DAVID website [32]. Data collected from the Real Time qRT-PCR was analyzed using the ΔΔCt method [33, 34].

Results

Cluster Analysis of Mixed Model Analyzed Data

For each individual MAP strain, mixed-model analyzed data was clustered with data from the other strains using Cluster 3.0 software, and associations were visualized via the Java Treeviewer (Figure 2.1) [31]. Figure 2.1 thus illustrates how closely related the various MAP strains are to each other, based on similarities in how they affect the host macrophage's transcriptome. Notably, there is little to no species of origin based clustering for strains use in this study. However, there is close clustering between the two SuperShedder strains. Also, significant is the difference between the other MAP strains in our study and the commonly studied K10 strain. This difference was validated by using a strain generated by randomly switching data from previous microarrays and repeating the clustering . In this analysis, the difference between K10 and the other strains was preserved (Data not shown). Additionally,

when the composite strain was added into cluster analyses the 5001 strain clustered most closely to the composite strain (Data not shown). Clustering revealed two major clades of MAP strains separated on how they affected host macrophage transcriptome (Figure 2.1). Based on these results representative strains (ATCC 19698 and 1018) were selected from the two major clades for validation studies using Real Time qRT-PCR (Figure 2.1). These strains share the same species of origin so this variable was removed from consideration.

Reannotations of the BOTL5 Microarray

In order to analyze results from this study, the BOTL5 microarray was reannotated using the most up to date human and bovine sequences available. The latest versions of the human, bovine, and Non-Redundant (NR) protein databases were downloaded on March 23, 2009 along with the most recent version of BLAST from the NCBI FTP database. This study used basic blast parameters and parsed the top hit in each BLAST search. While individual alignments were previously performed to study what known sequences are present on the BOTL5 microarray, these alignments left many sequences noted as being unknown. To rectify this problem, the BOTL5 microarray was reannotated using several genomes. As human is the most well annotated sequence available for mammals, all sequences were ultimately aligned to human sequences to utilize the available human data. The first alignment consisted of comparing BOTL5 cDNA sequences against human protein sequences. cDNA sequences that did not show any significant alignment to human protein sequences were then aligned against the bovine protein database. Conversely, bovine protein database sequences that had significant alignment with BOTL5 cDNA sequences were aligned with sequences in the human protein database. BOTL5 cDNA sequences that did not align with the known bovine proteins or BOTL5 cDNA aligned bovine sequences that did not match with human sequences were then aligned with the

sequences in the NR protein database. Again to identify more information about these sequences, the NR proteins with significant alignment to the BOTL5 cDNA were aligned to the human protein database. By this method, 1015 genes were identified as being present on the BOTL5 microarray out of a total of 1397 sequences. This is a vast improvement over the old annotations, which listed only 800 known genes on this microarray resource. The most recent human and bovine annotations of the BOTL5 microarray are present on the Center for Animal Functional Genomics website (http://www.cafg.msu.edu).

Statistical Analysis of Microarray Results

This study used PBMCs isolated from five Holstein cattle. To reduce the amount of cow to cow variability and emphasize variations caused by MAP infection, a mixed model approach was used to analyze the data. Using this method, 91 array features were found on average to be significantly differently expressed between infected MDMs compared to uninfected MDMs ($P \leq 0.01$). Of these features on the BOTL5 microarray, 78 had significant annotations based on the previously described annotation section (TABLE 2.1). Of the remaining 13 array features, all had alignments to the bovine genome indicating that these sequences are not random contaminants on the microarray. However, since nothing is known about these sequences, they were excluded from further analysis. Of the 78 annotated sequences shown to be significantly differentially expressed in MAP infected MDM cells, relative to uninfected cells, only 5 have been previously studied in mycobacterial infections (Table 2).

DAVID Analysis of Differentially Expressed Host Genes in MAP Infection

To better study trends of differentially expressed genes in MAP infection, the 78 significant genes from microarray analyses were studied using the DAVID analysis program.

DAVID assesses if a gene set (differentially regulated in MAP infection) contains an over-representation of genes in any given functional category, relative to the overall microarray. For this analysis, all annotated genes on the BOTL5 microarray were used as a background to measure enrichment in functional groupings. In this analysis, the most significant group was genes in the caspase (apoptosis) pathway (p value ≤ 0.0011). This group contained 5 genes and was enriched 8.4 times in our differentially regulated gene set, relative to the overall BOTL5 microarray. The largest group of genes showing significant enrichment in our differentially regulated set belonged to the metabolic pathway (p value ≤ 0.042). This group contained 44 genes and was enriched 1.2 times relative to the overall BOTL5 microarray. A more complete table of significantly enriched functional categories is provided in TABLE 2.3.

Real Time qRT-PCR analysis of Selected Differentially Expressed Host Genes in MAP infection

Based on microarray results, previous knowledge of genes involved in mycobacterial infection, and information from the published literature about each of the individual genes, several host genes were selected for validation of differential expression via Real Time qRT-PCR. Genes involved in apoptosis, immune system regulation, vacuole maintenance and surface membrane regulators, and proteins shown to be involved in signal reception and signal mediation were selected.

As the most significant functional area indicated by the DAVID analysis, several apoptosis genes were also selected for validation. Evaluation of Caspase 4 (CASP4) and poly (ADP-ribose) polymerase 1 (PARP1) expression showed infection with both representative strains of MAP caused a ~2.5-fold increase in CASP4 mRNA and a ~2-fold decrease in PARP1 mRNA relative to control uninfected cells, respectively (Figure 2.2). These differences were

significant when compared to controls ($p < 0.01$ for CASP4 and $p < 0.02$ for PARP1). Caspase 1 (CASP1) mRNA was also shown to be significantly up-regulated relative to control ($p = 0.03$) in ATCC infected cells while only showing a trend toward significant up-regulation of mRNA in 1018 infected MDMs ($p = 0.05$). Infection with both strains caused approximately a 2-fold increase in CASP1 mRNA expression (Figure 2.2). In contrast, Caspase 3 (CASP3) and DNA Fragmentation Factor, alpha (DFFA) expression was shown to be significantly down-regulated in 1018 infected macrophages (fold change = -1.89 and $p < 0.001$ for CASP3 and fold change = -1.56 and $p < 0.03$ for DFFA). In contrast, ATCC infection of MDM showed no significant differences in expression of either CASP3 or DFFA mRNA relative to controls (Figure 2.2). Evaluation of CASP6 showed no significant differences in expression following infection with either MAP strain (data not shown).

Another large functional group highlighted by our DAVID analysis of microarray data was receptors and signaling mediators. Real Time qRT-PCR of the AXL tyrosine kinase (AXL), Neuropilin 1 (NRP1), and Retinoid X Receptor, Alpha (RXRA) mRNA all showed a decrease in expression when MDM cells were infected with both representative MAP strains (Figure 2.3). This decrease in relative expression was significant when compared to uninfected controls ($p < 0.05$). Infection of MDM with strain 1018 also resulted in significant reduction in expression of fibroblast growth factor receptor 1 (FGFR1) and GATA binding protein 4 (GATA4) ($p < 0.05$). However, there was no significant expression difference for FGFR1 in ATCC infected macrophages while GATA4 showed a trend ($p < 0.06$) toward significant reduction in expression (Figure 2.3). Infection with either MAP strain did not result in significant differences in expression of nascent polypeptide-associated complex alpha subunit (NACA) from controls (data not shown).

Two genes (NFkB1 and mucosa associated lymphoid tissue lymphoma translocation gene 1, MALT1) whose expression was significantly different in MAP infected MDM cells relative to control MDM in the microarray analysis have previously been shown to be important in immune system regulation. Infection of MDM cells with both strains of MAP caused an ~3.7-fold increase in transcription of NFkB1 relative to control cells (Figure 2.4). Observed differences in NFkB1 transcription in both MAP strain infections were significant when compared to controls ($P < 0.01$). Expression of MALT1, however, was only shown to be significantly down-regulated in MDM infected with strain 1018 (fold change = -1.79, $p < 0.001$), relative to controls (Figure 2.4).

A final functional group containing many genes whose expression was significantly affected by MAP infection of MDM cells were genes involved in vacuole maintenance. Using Real Time qRT-PCR, ATPase, H+ transporting, lysosomal 70kDa, V1 subunit A (ATP6V0D1) expression was shown to be down-regulated in MDM following infection with strain 1018 (fold change = -1.3, $p < 0.05$). However, no changes in ATP6V0D1 expression were observed in MDM infected with the ATCC strain (Figure 2.5). Also, no significant differences from control were observed in expression of MMP16 or MMP23B genes following infection of MDM with either ATCC or 1018 strains (data not shown).

Real Time qRT-PCR analysis of Additional Host genes

In order to gain a better understanding of what cell death mechanisms might be altered in MAP infection of bovine macrophages, several apoptosis genes were selected for additional study. Expression of two pro-apoptotic genes, BCL2 antagonist of cell death (BAD) and TNF receptor 1 (TNFR1), were both down-regulated in MAP infected MDM cells relative to

uninfected cells (fold change -2.2 and -1.2 respectively). This decrease in transcription was shown to be significant in infection with both MAP strains ($p < 0.01$). No significant alterations in expression of TNF receptor 2 was observed in MDM cells infected with either MAP strain (data not shown).

To further elucidate what molecules are being produced by MAP infected macrophages that might facilitate communication with other immune cells, IL-1alpha, IL-1beta, BCL2, BCL2A1, IL-8, and MIP3alpha were selected for additional study. The expression of IL-1beta, IL-8, and MIP3alpha were all up-regulated in MDM cells infected with both strains of MAP, relative to uninfected control cells (Figure 2.5, 6, and 7). The increases in expression for all three genes were significant ($p < 0.02$) and were the largest increases in expression observed in the current study. IL-1alpha gene expression in MAP-infected MDM cells was shown to be significantly up-regulated in 1018 infection (fold change = ~23 over controls, $p < 0.001$). In MDM infected with the ATCC strain of MAP, the fold change was much lower (~13 fold over controls) and the data approached significance ($p < 0.11$, Figure 2.7). In the case of BCL2A1 gene expression in MAP-infected MDM, MDM infected with ATCC showed significant up-regulation of BCL2A1 (fold change = 8.1, $p < 0.03$), while MDM infected with the 1018 strain showed a similar fold change of 13 times the expression of BCL2A1 in uninfected MDM, the observed change only showed a trend to significance ($p < 0.06$, Figure 2.6). Lastly, BCL2 gene expression was shown to be significantly down-regulated in MDM infected with 1018 (fold change = -1.5, $p < 0.05$), while infection with ATCC showed no significant difference from uninfected controls (Figure 2.6).

Discussion

Little is known about the complex interaction between macrophages and mycobacteria. While a significant body of literature exists on *Mtb* interactions with host cells, there is a paucity of research on MAP- macrophage interactions. This study sought to find new candidate genes to better explain changes occurring in macrophages following infection with MAP. Of particular interest were mechanisms related to increased bacterial survival. The net result of this work was identification of 78 host genes/proteins that are possible targets for future work. Additionally, clustering MAP infection driven transcriptome changes in macrophages suggests some novel relationships. Through careful examination of individual genes and clustering results, a more thorough picture of what changes MAP infection induces in host macrophage cells can emerge. It is important to note that these results are from a population of infected and uninfected macrophages like many of the current microarray studies in the MAP-macrophage interaction field [26, 35, 36]. Recent research from a similar mycobacterium *Mycobacterium tuberculosis* has shown that very important differences exist between tuberculosis-infected and uninfected macrophages in these cultures and that infected tuberculosis-infected macrophages can vastly change the behavior of uninfected macrophages in the same culture [37].

Unbiased clustering using all genes displaying altered transcription following infection with all MAP strains also provided some unique outcomes. Chief among these results is the absence of species of origin related MAP strain clustering. Previous research has shown genetic differences between MAP strains isolated from cattle when compared to those from sheep. In general, sheep strains tend to be less virulent than cattle strains [27]. Our results suggest that this difference is likely an element of the particular MAP strain itself, rather than how these strains interact with host macrophages. While our infections were all performed in bovine MDMs isolated from uninfected cattle, we hypothesize that the observed differences between infected

and uninfected cell transcriptomes would be similar if this work were to be repeated using cells from other host species, such as sheep, deer, or even humans. MAP strains from both cattle and sheep can infect cells from several different animals and thus such comparison is entirely possible [38-40].

Another novel result from the cluster analysis was alignment of strains into three distinct groups, or clades. The first clade contained a single strain, K10. This MAP strain is often used as the sole strain for many MAP biology experiments. Our results suggest that the K10 MAP strain may not be the most representative for such studies. In support of this conclusion, Motiwala et al and Wu et al have shown that MAP strain K10 has several distinct genetic polymorphisms that clearly distinguish it from other MAP strains [41, 42]. This work highlights the fact that these genetic differences may drastically change the host response to infection. The second clade contained strains 1018, MAP5, MAP6, and 7565. The third clade contained MAP strains 7560, SS149, SS140, ATCC #19698, and 5001. The individual strains in the second and third clade are interesting and future work must be performed to see what host genes are responsible for the differences between these clades and if each MAP strain maintains these differences. A final result of note from the clustering analysis was a close relationship between the two SuperShedder strains used in this study. MAP strains SS140 and SS149 were both isolated from cattle exhibiting an extremely high level of MAP shedding in feces (R. Whitlock, personal communications). Currently, there is some debate on the nature and cause of the SuperShedding phenomena. In one hypothesis, SuperShedding is a result of the host response. Alternatively, the SuperShedding phenotype may be due to properties of the infecting strain. Further work to determine how these two strains affect host macrophages in similar ways and what separates these from the other strains will be of interest.

In terms of the individual genes studied, the largest functional group identified by DAVID analysis was genes encoding proteins involved in apoptosis. Initially this study found that expression of CASP3, CASP4, PARP1, GATA4, DFFA, CASP1, and CASP6 was significantly affected by MAP infection. After examination of the literature, BAD, TNFR1, TNFR2, BCL2, and BCL2A1 were added to this study. These results are entirely consistent with the literature as careful regulation of apoptosis related genes has been shown to be important in mycobacterial infection as well as intracellular survival of MAP [43]. While genes selected from the microarray data plus additional genes selected from the literature are not a complete picture of the "apoptosome", the distribution of these genes within the macrophage from the cytosol in the case of the caspases, the nucleus with DFFA and PARP1, and the mitochondria with BAD show that MAP infection alters the transcription of genes whose protein products act in many different cell compartments and demonstrates a general alteration in transcription of apoptosome genes. Regulation of the host cell apoptosome presents two hypotheses, which are equally supported by current literature. If an infected cell is able to trigger apoptosis then the intracellular bacteria will be collected in cellular blebs and phagocytosed by other macrophages, allowing destruction of the bacteria, much like what is seen in *Mtb* [44]. Conversely, if MAP is able to prevent apoptosis then the bacteria can survive and proliferate while still avoiding detection by the immune system, again much like what is observed in *Mtb* [45].

Differences in apoptosis gene expression based on infecting MAP strain were observed in Real Time qRT-PCR. For example, macrophages infected with strain 1018 showed significant down-regulation of DFFA and CASP3, while infection with the ATCC strain did not significantly change expression of these genes relative to control cells. As these two genes have opposite affects on cell apoptosis (pro apoptosis for CASP3 and anti apoptosis for DFFA), no

clear cut explanation can be drawn from MAP infection driven regulation of these genes [46, 47]. As CASP3 has been shown to directly cleave DFFA into an inactive form, this may indicate a general down-regulation of late-state apoptosis genes in 1018 infected macrophages [46].

In addition to the role CASP1 and CASP4 play in apoptosis, they also play an important role in processing cytokines for communication with other immune system cells. While not highly significant in Real Time qRT-PCR studies using MDM infected with strain 1018 and the ATCC strain, an overall trend in MAP infection was an increase in transcription for both CASP1 and CASP4. CASP4 has been shown to cleave its own precursor as well as the CASP1 precursor [48]. In addition to CASP4 cleavage of CASP1, CASP1 has been shown to autocatalytically leave its own precursor as well as IL-1beta from its precursor forms [49]. Enhanced expression of IL-1 in MAP infected macrophages is consistent with previous results [9]. It has been suggested that some late effects of Johne's disease, such as inflammatory damage to the host, may be due to drastic over-expression of IL-1 by MAP-infected intestinal macrophages [9, 25].

The importance of cytokine processing and networks in response to MAP infection suggested by altered CASP1 and CASP4 expression is further highlighted by increased transcription of genes encoding NF-kB1, MIP3alpha, and MALT1. NF-kB1 is an important transcription factor regulating many immune function genes and is directly involved in IL-1 activation [50]. MALT1 may play a secondary role in IL-1 transcription increases following MAP infection by activating NF-kB1 [51]. MIP3alpha is transcribed when NF-kB1 is activated in *Mtb* infection [52]. Enhanced expression of NF-kB1 in MAP-infected macrophages combined with increased expression of NFkB1 activators MIP3alpha and MALT1 could explain the increase in IL-1 and its processing enzymes, eventually leading to IL-1 inflammatory-driven damage of the host as previously theorized [9, 25].

Another area of special consideration and at the intersection of immune system communication and apoptosis is expression of TNFR1 and TNFR2 in MAP-infected cells. MAP infection resulted in decreased mRNA expression for TNFR1, regardless of infecting strain, while no changes in TNFR2 transcription were observed in infected macrophages. TNFR1 has been implicated as the more pro-apoptotic of the two TNFalpha receptors, while TNFR2 has been linked to suppression of apoptosis. If cell surface expression of TNFR2 remains constant while TNFR1 is reduced, then MAP infection may cause cells to persist while uninfected cells recruited to the area may undergo apoptosis, particularly in the face of enhanced local TNFalpha concentrations. This theory is supported by a recent computation theory paper studying the role TNFalpha has in *Mtb* granuloma formation that shows removal of TNFalpha mediated cell death resulted in increased clearance of the bacteria from the experimental system [53].

While several signal mediators and receptors were found to be alternatively expressed in MAP-infected MDM cells, a gene of particular interest is AXL and its possible role in Crohn's disease's apparent autoimmunity. Our data showed a down-regulation of AXL expression in MAP-infected macrophages (Figure 2.3). In AXL knock-out mice that also have knock-outs in similar related genes, B and T cells over proliferate eventually leading to the development of autoimmune disorders [54]. Of Interest, Crohn's disease is currently classified as an autoimmune disease[55]. Taken together these facts could explain the development of an ineffective humoral immune response in Johne's disease and the possible observation of an autoimmune disease being associated with Crohn's disease. These two separate disease factors may be the result of MAP infection of macrophages causing down-regulation of AXL and related gene expression. While the MAP biology community is somewhat divided on if MAP is the causative agent of Crohn's disease, it is tempting to speculate that the over proliferation of B and

T cells observed in Crohn's and the eventual ineffective humoral response observed in Johne's disease may be caused by same event, down-regulation of AXL family expression in MAP-infected macrophages [56].

Perhaps the least intuitive genes in this study were some of the signal receptors. Genes such as RXRA, FGFR1, and NRP1 have not been previously studied in mycobacterial infection of macrophages. What role these genes may play in infection is unclear at present. While NRP1 was down-regulated in MAP-infected macrophages in this study, NRP1's role in the infected cell is difficult to discern. Previous siRNA reduction experiments have shown removing this transcript does not overtly affect the cell, indicating that NRP1 may not be necessary for cell maintenance [57]. In contrast, FGFR1 has been implicated in NF-kB1 signaling, linking this gene back to communication in the immune system [58]. One commonality among these genes is that they are all down-regulated in MAP infection. Since down-regulation of growth factor receptor expression is implicated as either a cause or direct effect of apoptosis, a decrease in transcription of these growth factor receptor genes may promote or prevent cell death in infected macrophages. Recently, research on the Liver X Receptor (LXR) has shown that LXRs are necessary for proper activation of macrophages and lead to destruction of intracellular Mtb [59]. LXRs also form heterodimers with RXRs, possibly implicating this receptor in macrophage Mtb control [60]. If FGFR1 and NRP1 also bind receptors that are important to intracellular mycobacteria control, then down-regulation of these genes may be an important step for the bacterial to survival in the phagosome.

Another interesting single gene found in this study was ATP6V0D1, a gene involved in vacuole maintenance. While little is known about this gene, ATP6V0D1 has been shown to be involved in acidification of lysosomes [61]. Failure of the endosome to acidify is currently

thought to be part of the MAP intracellular survival mechanism [62] . Data from this study indicates that expression of this gene is down-regulated following MAP infection of MDM cells. Based on this information, MAP infection possibly prevents transcription of ATP6V0D1 through an as yet unknown mechanism and by preventing acidification halts MAP-carrying endosome fusion with mature lysosomes.

This study sought to elucidate some of the complex interactions between MAP bacteria and the bovine host macrophage. Using BOTL5 microarrays and 10 distinct MAP strains to measure relative gene expression between MAP-infected and uninfected cells, common patterns of gene expression were observed as well as novel clusters of MAP strains. When the total transcriptome alterations in MAP-infected macrophages were examined, K10 was observed as an outlier and SuperShedding MAP strains were observed to cluster together. A total of 78 annotated bovine genes were found to be differentially expressed in MAP infected macrophages, relative to uninfected cells. Many of these genes have never been studied in the context of mycobacterial infection. Within the group of differentially expressed genes, significant enrichment in genes encoding proteins involved in apoptosis was found to have altered expression. To validate the results of the microarray study, many of the 78 genes were also found to have altered expression in MAP infected cells via Real Time qRT-PCR. While no clear pattern of apoptosis gene expression emerged from the data, MAP infection of MDM cells does modulate large portions of the infected host apoptosome. Additionally, differences in cytokine gene processing and regulation were observed that mimic previously reported results in related mycobacteria. Finally, a large contingent of growth factor receptors that have not been studied in bacterial infection have now been implicated as important in MAP infection and intracellular survival. Further more focused studies of what roles these genes play in MAP infection of host

macrophages are necessary to better determine what benefit transcriptional regulation of these transcripts confer to either the infecting MAP bacteria or the host.

.BOTL ID	FDR	REFSEQ Protein ID	Name	Abbreviation	Function
BOTL0100011_E01	5.95E-08	NP_006787	AFG3 ATPase family gene 3-like 2 (yeast)	AFG3L2	Unknown
BOTL0100003XE07R	1.79E-07	NP_004981	methionyl-tRNA synthetase	MARS	Charging tRNAs with amino acids
BOTL0100010_G01	2.83E-07	NP_000150	glutaryl-Coenzyme A dehydrogenase	GCDH	Degradation of Amino Acids
BOTL0100010_F10	4.08E-06	NP_002687	Polymerase (RNA) II (DNA directed) polypeptide G	POLR2G	Initiation and stabilization of transcription
BOTL0400190_PCR	5.36E-06	NP_998731	DNA fragmentation factor, 45kDa, alpha polypeptide	DFFA	Repression of Apoptosis
BOTL0100011_A03	7.01E-06	XP_001128076	hypothetical LOC728174	LOC728174	Unknown
BOTL0100010_C12	1.02E-05	NP_570115	GTPase, IMAP family member 1	GIMAP1	Unknown
BOTL0400179_PCR	1.27E-05	NP_001217	caspase 6, apoptosis-related cysteine peptidase	CASP6	Activation of downstream caspase cascade
BOTL0100010_F08	2.35E-05	NP_659425	asparagine-linked glycosylation 14 homolog (S. cerevisiae)	ALG14	Involved in N-Glycan biosynthesis
BOTL0100009_G08	2.39E-05	NP_005185	CCAAT/enhancer binding protein (C/EBP), beta	CEBPB	Transcription factor

TABLE 2.1

TABLE 2.1 (Cont'd)

BOTL0100013_A06	2.39E-05	NP_612392	metastasis suppressor 1-like	MTSS1L	Unknown
BOTL0100008_C03	2.40E-05	NP_002963	SET binding factor 1	SBF1	Prevention of dephosphorilation
BOTL0400648_PCR	2.57E-05	NP_068713	AXL receptor tyrosine kinase	AXL	Stimulation of cell proliferation
BOTL0400077_PCR	3.73E-05	NP_003937	nucleolar protein 3 (apoptosis repressor with CARD domain)	NOL3	Regulation of Apoptosis
BOTL0100003XF12R	4.27E-05	NP_001681	ATPase, H+ transporting, lysosomal 70kDa, V1 subunit A	ATP6V0D1	Acidification of intracellular organelles
BOTL0400105_PCR	6.32E-05	NP_001707	Chemokine (C-X-C motif) receptor 5	CXCR5	Migration and localization of B Cells
BOTL0100009_A11	8.47E-05	NP_003725	amine oxidase, copper containing 3 (vascular adhesion protein 1)	AOC3	Conversion of amines to aldehydes
BOTL0400139_PCR	9.94E-05	NP_001216	caspase 4, apoptosis-related cysteine peptidase	CASP4	Induction of Apoptosis and protolysis
BOTL0400388_PCR	0.000154	NP_004751	serine/threonine kinase 17a	STK17A	Induction of Apoptosis
BOTL0100003XH07R	0.000182	NP_775918	ring finger protein 149	RNF149	Unknown
BOTL0400342_PCR	0.000182	NP_057021	phosphatidylinositol glycan anchor biosynthesis, class T	PIGT	glycosylphosphatidylinositol-anchor biosynthesis
BOTL0100008_B03	0.000225	NP_116246	lactamase, beta	LACTB	Mitochondrial ribosome subunit

TABLE 2.1 (Cont'd)

BOTL0400360_PCR	0.000299	NP_005932	matrix metallopeptidase 16 (membrane-inserted)	MMP16	Degradation of extracellular matrix
BOTL0400511_PCR	0.000299	NP_002731	protein kinase C, iota	PRKCI	Regulation of Apoptosis
BOTL0100009_F03	0.000344	NP_056203	Yip1 domain family, member 3	YIPF3	Unknown
BOTL0400518_PCR	0.000427	NP_001019799	neuropilin 1	NRP1	Coreceptor for vascular endothelial growth factor and semaphorin
BOTL0100011_D10	0.000427	NP_054872	zinc finger CCCH-type containing 7A	ZC3H7A	Unknown
BOTL0100007_H05	0.000507	NP_008826	histamine N-methyltransferase	HNMT	Metabolism of histamine
BOTL0400451_PCR	0.00063	NP_002574	PRKC, apoptosis, WT1, regulator	PAWR	Repressor of transcription
BOTL0400585_PCR	0.000862	NP_150634	caspase 1, apoptosis-related cysteine peptidase (interleukin 1, beta, convertase)	CASP1	Induction of Apoptosis and protolysis
BOTL0400001_PCR	0.000862	NP_005364	myeloproliferative leukemia virus oncogene	MPL	Kinase
BOTL0100009_F09	0.000999	NP_005868	splicing factor 3a, subunit 1, 120kDa	SF3A1	Splicing pre-mRNA
BOTL0100010_F04	0.001033	NP_660203	proline-rich acidic protein 1	PRAP1	Regulation of cell proliferation

TABLE 2.1 (Cont'd)

BOTL0100009_B10	0.001049	NP_640334	FYVE, RhoGEF and PH domain containing 4	FGD4	Regulation of cytoskeleton and cell shape
BOTL0100010_C09	0.001141	NP_001005746	Calcium channel, voltage-dependent, beta 4 subunit	CACNB4	Mediates calcium intake in cells
BOTL0400626_PCR	0.00125	NP_003246	TIMP metallopeptidase inhibitor 2	TIMP2	Inhibition of Matrix Metaloprotiase
BOTL0100013_H01	0.001256	NP_003033	Solute carrier family 6 (neurotransmitter transporter, GABA), member 1	SLC6A1	Transport of GABA into and out of cells
BOTL0100010_C05	0.00134	NP_077001	dCTP pyrophosphatase 1	DCTPP1	Unknown
BOTL0100003XG10R	0.001359	NP_002948	retinoid X receptor, alpha	RXRA	Regulation of transcription
BOTL0100008_H06	0.00136	NP_056194	brain protein I3	BRI3	Regulation of Apoptosis
BOTL0100012_D09	0.001395	NP_001006936	transcription elongation factor A (SII)-like 4	TCEAL4	Modulation of transcription
BOTL0400362_PCR	0.001549	NP_008914	matrix metallopeptidase 23B	MMP23B	Degradation of extracellular matrix
BOTL0400544_PCR	0.001549	NP_001609	poly (ADP-ribose) polymerase 1	PARP1	Apoptosis initiation and DNA repair
BOTL0400322_PCR	0.001699	NP_000221	Leptin	LEP	Inhibition of food intake

TABLE 2.1 (Cont'd)

BOTL0400470_PCR	0.001812	NP_003122	serum response factor (c-fos serum response element-binding transcription factor)	SRF	Stimulates cell proliferation and differentiation
BOTL0100008_C06	0.001835	NP_006433	DR1-associated protein 1 (negative cofactor 2 alpha)	DRAP1	Repressor of transcription
BOTL0100001XD10R	0.001932	NP_001106672	nascent polypeptide-associated complex alpha subunit	NACA	Regulation of cell differentiation
BOTL0100011_B07	0.002223	NP_570115	GTPase, IMAP family member 1	GIMAP1	Unknown
BOTL0100003XF01R	0.002553	NP_004638	D4, zinc and double PHD fingers family 1	DPF1	Unknown
BOTL0400243_PCR	0.003318	NP_002043	GATA binding protein 4	GATA4	Transcription factor
BOTL0100009_H01	0.003569	NP_477517	loss of heterozygosity, 12, chromosomal region 1	LOH12CR1	Unknown
BOTL0400631_PCR	0.004159	NP_114425	interferon, alpha-inducible protein 27-like 2	IFI27L2	Unknown
BOTL0100001XD07R	0.004393	NP_060277	O-sialoglycoprotein endopeptidase	OSGEP	Unknown
BOTL0400542_PCR	0.004597	NP_148983	platelet-derived growth factor alpha polypeptide	PDGFA	Cell differentiation
BOTL0400481_PCR	0.004714	NP_690619	PTK7 protein tyrosine kinase 7	PTK7	Adhesion and signal transduction

TABLE 2.1 (Cont'd)

BOTL0100012_C09	0.004714	NP_079083	triggering receptor expressed on myeloid cells-like 2	TREML2	Unknown
BOTL0100001XE12R	0.004766	NP_000588	insulin-like growth factor binding protein 2, 36kDa	IGFBP2	Unknown
BOTL0100006XF03R	0.005246	NP_056969	PCF11, cleavage and polyadenylation factor subunit, homolog (S. cerevisiae)	PCF11	RNA regulation
BOTL0100008_F08	0.005249	NP_001017923	Chromosome 14 open reading frame 28	C14orf28	Unknown
BOTL0400227_PCR	0.005592	NP_075598	fibroblast growth factor receptor 1	FGFR1	Signal transduction for differentiation
BOTL0100010_C10	0.005592	NP_055990	neurobeachin-like 2	NBEAL2	Unknown
BOTL0100004XC03R	0.005659	NP_055395	solute carrier family 2 (facilitated glucose transporter), member 8	SLC2A8	Hexose transport
BOTL0100010_B09	0.005742	NP_057629	immediate early response 5	IER5	Mediation of mitogenic signals
BOTL0100009_F10	0.006042	NP_776216	mucosa associated lymphoid tissue lymphoma translocation gene 1	MALT1	Possible activation of NF-kB
BOTL0100004XC08R	0.00701	NP_536858	protein tyrosine phosphatase, non-receptor type 6	PTPN6	Regulation of signaling in hematopoietic cells

TABLE 2.1 (Cont'd)

BOTL0100001XE09R	0.007219	XP_001723453	similar to prothymosin alpha	LOC643287	Unknown
BOTL0100013_E08	0.007552	NP_062456	motile sperm domain containing 1	MOSPD1	Unknown
BOTL0400078_PCR	0.007552	NP_003937	nucleolar protein 3 (apoptosis repressor with CARD domain)	NOL3	Repressor of apoptosis
BOTL0100003XF05R	0.008042	NP_113688	protocadherin alpha 4	PCDHA4	Establishment and function of cell-cell connections
BOTL0100003XG06R	0.008246	NP_001597	ATP-binding cassette, sub-family A (ABC1), member 2	ABCA2	Lipid metabolism and neural development
BOTL0100009_G04	0.008367	NP_055830	lysine (K)-specific demethylase 4B	KDM4B	Unknown
BOTL0100009_E04	0.008459	NP_004350	cell division cycle 34 homolog (S. cerevisiae)	CDC34	Regulation of Cell cycle regulators
BOTL0400335_PCR	0.008545	NP_079080	zinc finger protein 669	ZNF669	Unknown
BOTL0100011_C07	0.008687	XP_001718345	similar to hydroxyproline-rich glycoprotein VSP-3	LOC100129104	Unknown
BOTL0400348_PCR	0.008719	NP_066286	chemokine (C-C motif) ligand 3-like 1	CCL3L1	Secreted immunoregulatory protein
BOTL0100013_A08	0.009199	NP_001035364	synaptonemal complex protein 2-like	SYCP2L	Unknown

TABLE 2.1 (Cont'd)

BOTL0400219_PCR	0.009571	NP_000790	erythropoietin	EPO	Promotes cells differentiation and hemoglobin synthesis
BOTL0100010_E07	0.009846	NP_057356	transducer of ERBB2, 2	TOB2	Regulation of cell cycle progression

TABLE 2.1 BOTL5 genes discovered to have altered expression in MAP infection The above table shows what genes had altered expression in MAP infection. The first column indicates the name of the feature on the BOTL5 microarray. The FDR column indicates the P value of each gene after false discovery rate calculation. The REFSEQ Protein ID column indicates what Human REFSEQ protein is linked to each spot. The name column indicates the proper name for each gene on the microarray. The abbreviation column indicates the abbreviation of each gene. The Function column gives a short summary of the function of each gene. These function are abbreviated OMIM and GENE databases references [63].

REFSEQ Identifier	Full Name	Abbreviation	Original Publication
NP_001707	chemokine (C-X-C motif) receptor 5	CXCR5	Patterns of chemokine receptor expression on peripheral blood gamma delta T lymphocytes: strong expression of CCR5 is a selective feature of V delta 2/V gamma 9 gamma delta T cells. Glatzel A et al[64]
NP_150634	caspase 1, apoptosis-related cysteine peptidase (interleukin 1, beta, convertase)	CASP1	Apoptosis of Mycobacterium avium-infected macrophages is mediated by both tumor necrosis factor (TNF) and Fas, and involves the activation of caspases. Bermudez LE et al.[65]
NP_000221	leptin	LEP	Pulmonary Mycobacterium tuberculosis infection in leptin-deficient ob/ob mice. Wieland CW et al.[66]
NP_776216	mucosa associated lymphoid tissue lymphoma translocation gene 1	MALT1	Adjuvanticity of a synthetic cord factor analogue for subunit Mycobacterium tuberculosis vaccination requires FcRgamma-Syk-Card9-dependent innate immune activation. Werninghaus K et al.[67]
NP_000790	Erythropoietin	EPO	Preferential differentiation of hematopoietic stem cells in mice after intravenous injection of BCG Marchal G.[68]

Table 2.2 Previously Studied Host Genes The above table shows genes that have previously been studied in MAP infection with the host. These experiments vary from cell culture experiments to full animal studies. The first column is the REFSEQ-Protein Identifier. The second and third columns are the name of the protein and its abbreviation. The third column is the title of the original research that studied this gene in the context of MAP interaction and the original authors.

Category	Term	Count	PValue	Fold Enrichment
GOTERM_MF_ALL	GO:0016787~hydrolase activity	16	0.009341	1.937046
CGAP_SAGE_QUARTILE	35:ovary_serous adenocarcinoma_3rd	18	0.022052	1.690196
GNF_U133A_QUARTILE	Pituitary_3rd	19	0.029467	1.591401
GOTERM_MF_ALL	GO:0030693~caspase activity	4	0.006192	9.039548
CGAP_SAGE_QUARTILE	42:brain_glioblastoma, cerebral cortex_3rd	16	0.036364	1.676228
GOTERM_MF_ALL	GO:0003824~catalytic activity	31	0.023327	1.364737
SP_COMMENT	similarity:Belongs to the peptidase C14 family.	4	0.003212	10.86792
GOTERM_MF_ALL	GO:0022804~active transmembrane transporter activity	4	0.039313	4.930663
GOTERM_MF_ALL	GO:0004197~cysteine-type endopeptidase activity	4	0.049766	4.519774
CGAP_SAGE_QUARTILE	127:pancreas_primary adenocarcinoma_3rd	19	0.031229	1.595053

TABLE 2.3

TABLE 2.3 (Cont'd)

CGAP_EST_QUARTILE	38108:mammary gland_neoplasia_3rd	6	0.02977	3.236295
CGAP_SAGE_QUARTILE	41:brain_glioblastoma, cerebral cortex_3rd	18	0.037469	1.59564
SP_PIR_KEYWORDS	Zinc	13	0.035648	1.833562
UNIGENE_EST_QUARTILE	soft tissue/muscle tissue tumor_disease_3rd	22	0.026423	1.530061
GOTERM_MF_ALL	GO:0008233~peptidase activity	9	0.013722	2.652911
UNIGENE_EST_QUARTILE	skin_normal_3rd	22	0.028028	1.521791
CGAP_SAGE_QUARTILE	177:mammary gland_breast carcinoma cell line_3rd	16	0.047238	1.622588
INTERPRO	IPR001309:Caspase, p20 subunit	4	0.003664	10.43871
SP_PIR_KEYWORDS	Protease	7	0.025654	2.900202
GOTERM_MF_ALL	GO:0004175~endopeptidase activity	8	0.020446	2.711864
SEQUENCE_LENGTH	414	3	0.017012	12.66176
BIOCARTA	h_caspasePathway:Caspase Cascade in Apoptosis	5	0.001064	8.398693
CGAP_SAGE_QUARTILE	67:brain_glioblatastoma infected with LacZ control, cerebral cortex_3rd	17	0.019794	1.752033

TABLE 2.3 (Cont'd)

GOTERM_BP_ALL	GO:0006508~proteolysis	9	0.026984	2.358012
GOTERM_BP_ALL	GO:0030031~cell projection biogenesis	3	0.046031	8.017241
GOTERM_BP_ALL	GO:0008152~metabolic process	44	0.041408	1.18296
GNF_U133A_QUARTILE	Adrenal Cortex_3rd	20	0.034089	1.538012
INTERPRO	IPR011600:Peptidase C14, caspase catalytic	4	0.003664	10.43871
COG_ONTOLOGY	Posttranslational modification, protein turnover, chaperones	3	0.046326	6.875
CGAP_EST_QUARTILE	21358:lung_neoplasia_3rd	4	0.049849	4.511199
PUBMED_ID	10069390	3	0.017157	12.61429
GOTERM_MF_ALL	GO:0008270~zinc ion binding	14	0.022135	1.87951
INTERPRO	IPR002138:Peptidase C14, caspase non-catalytic subunit p10	3	0.030408	9.78629
INTERPRO	IPR002398:Peptidase C14, caspase precursor p45	3	0.048238	7.829032

TABLE 2.3 DAVID analysis The above table shows the significantly enriched functional categories from the DAVID analysis of the 78 known genes. The first column Category indicates category the functional grouping originates from. The second column Term shows the subcategory that is enriched from the main grouping. The Number category indicates the number of genes in each category.

The P-value indicates how significant each result is. The final category Fold Enrichment show how enriched over background each functional category is.

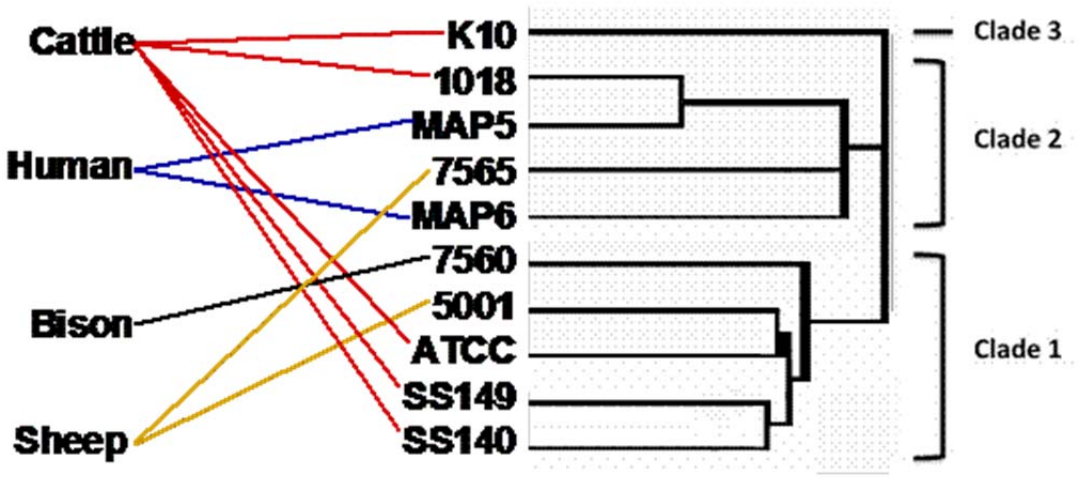

Figure 2.1 Cluster Analysis of Host Gene Expression induced by various MAP strains. The above clustering was performed using the resulting single strain data from the mix-model analysis of all the features on the BOTL5 microarray. Lines indicate the species of origin each MAP strain was harvest from. Of note, three separate clades were observed with K10 as its own clade. Also, note no species of origin clustering was observed in these results. For interpretation of the references to color in this and all other figures, the reader is referred to the electronic version of this dissertation.

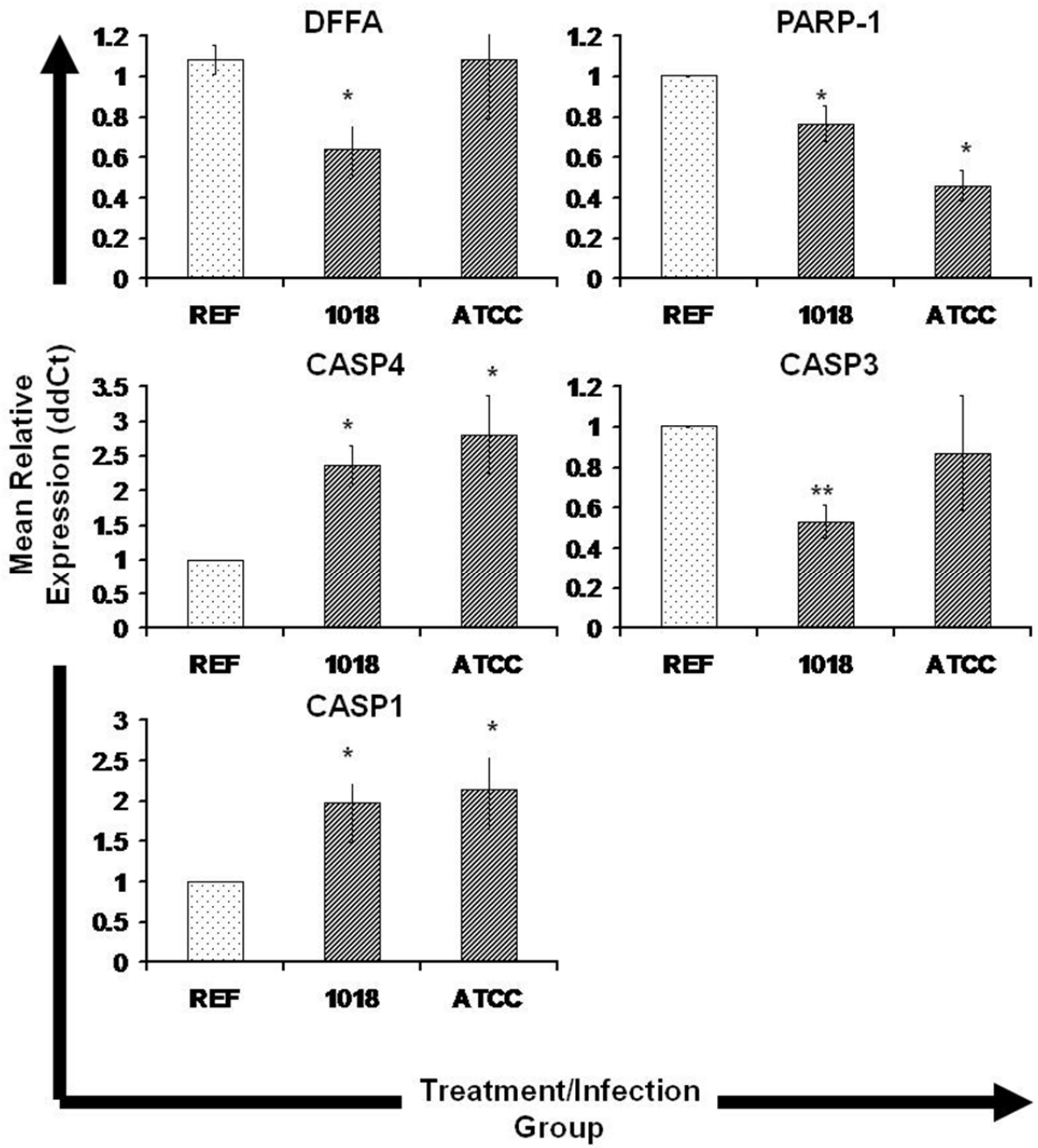

Figure 2.2-Expression of apoptosis genes in mature MDM cells following infection with MAP. Gene expression was assessed by Real Time qRT-PCR as previously described. Data was analyzed via the ddCt method using beta-actin as the control gene. The uninfected sample (REF) is indicated by the dotted sample while infected samples are shown with slashing lines. The bars represent the average results of MDM cultured from six animals. Error bars represent

SE between the six biological replicates. * indicates significantly different from controls at a $p < 0.05$ and ** indicates significantly different from controls at $p < 0.01$.

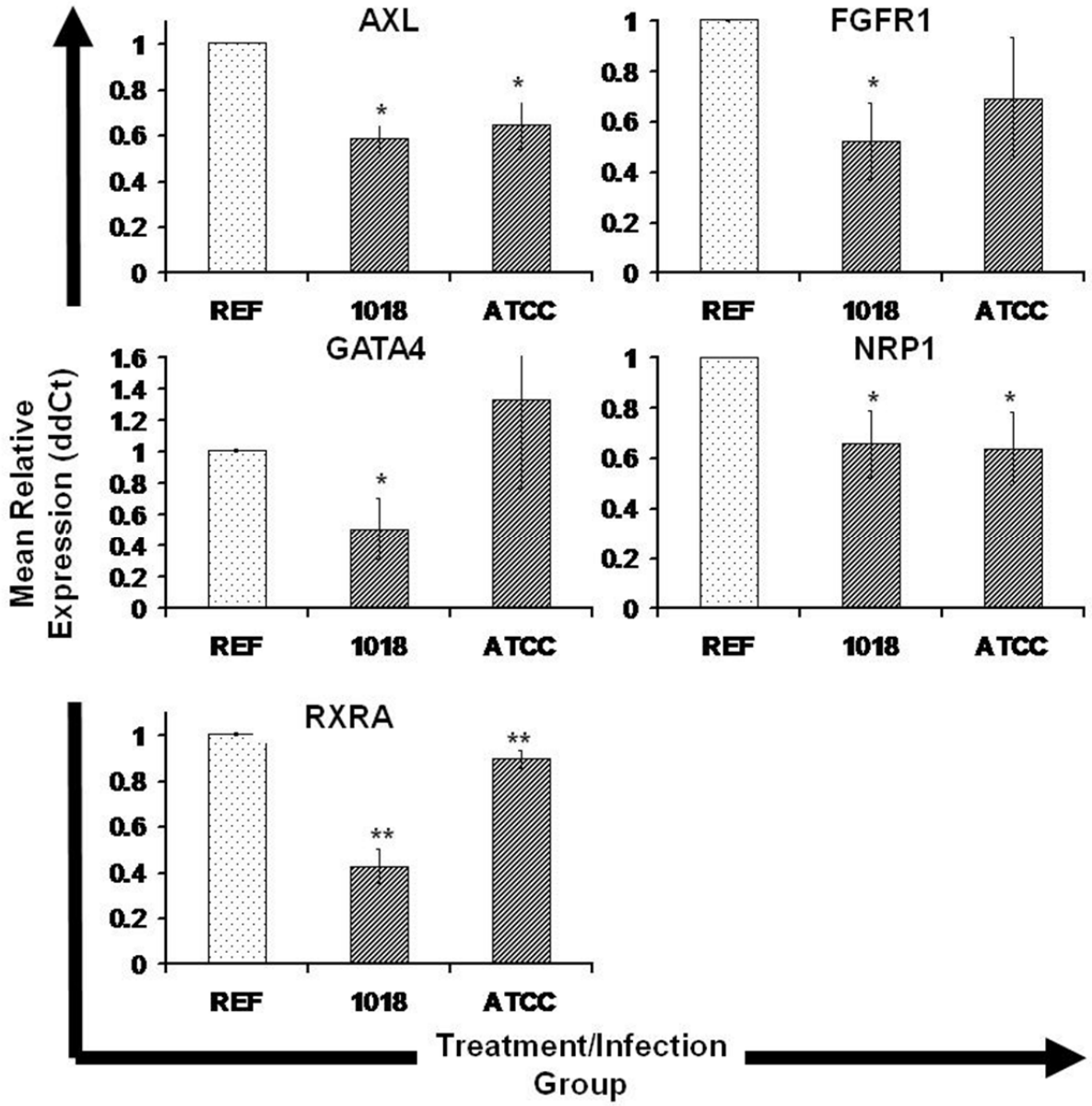

Figure 2.3-Expression of transcription factors in mature MDM cells following infection with MAP. Gene expression was assessed by Real Time qRT-PCR as previously described. Data was analyzed via the ddCt method using beta-actin as the control gene. The uninfected

sample (REF) is indicated by the dotted sample while infected samples are shown with slashing lines. The bars represent the average results of MDM cultured from six animals. Error bars represent SE between the six biological replicates. * indicates significantly different from controls at a $p < 0.05$ and ** indicates significantly different from controls at $p < 0.01$.

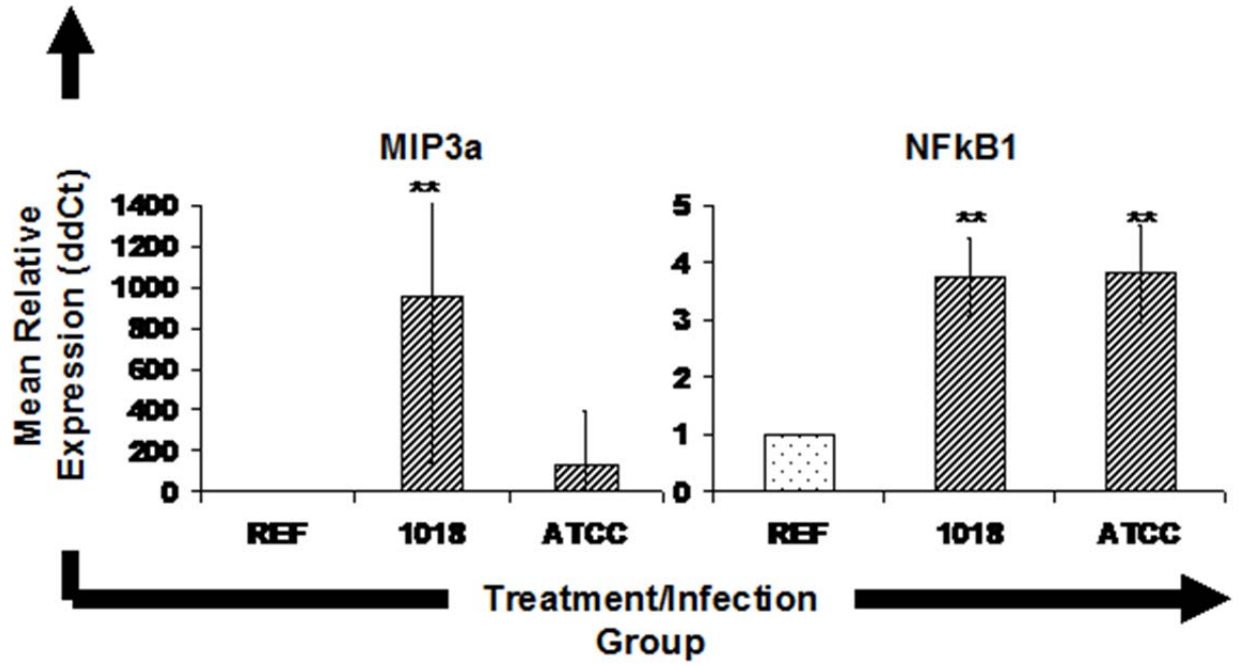

Figure 2.4-Expression of immune signaling genes in mature MDM cells following infection with MAP. Gene expression was assessed by Real Time qRT-PCR as previously described. Data was analyzed via the ddCt method using beta-actin as the control gene. The uninfected sample (REF) is indicated by the dotted sample while infected samples are shown with slashing lines. The bars represent the average results of MDM cultured from six animals. Error bars represent SE between the six biological replicates. * indicates significantly different from controls at a $p < 0.05$ and ** indicates significantly different from controls at $p < 0.01$.

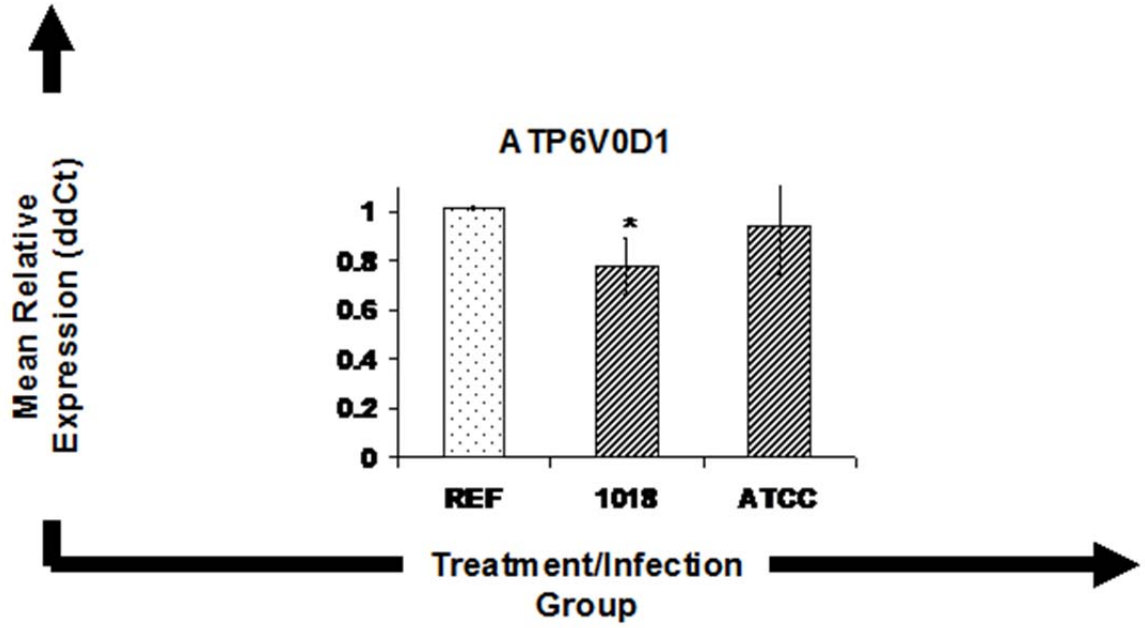

Figure 2.5-Expression of vacuole and surface genes in mature MDM cells following infection with MAP. Gene expression was assessed by Real Time qRT-PCR as previously described. Data was analyzed via the ddCt method using beta-actin as the control gene. The uninfected sample (REF) is indicated by the dotted sample while infected samples are shown with slashing lines. The bars represent the average results of MDM cultured from six animals. Error bars represent SE between the six biological replicates. * indicates significantly different from controls at a $p < 0.05$ and ** indicates significantly different from controls at $p < 0.01$.

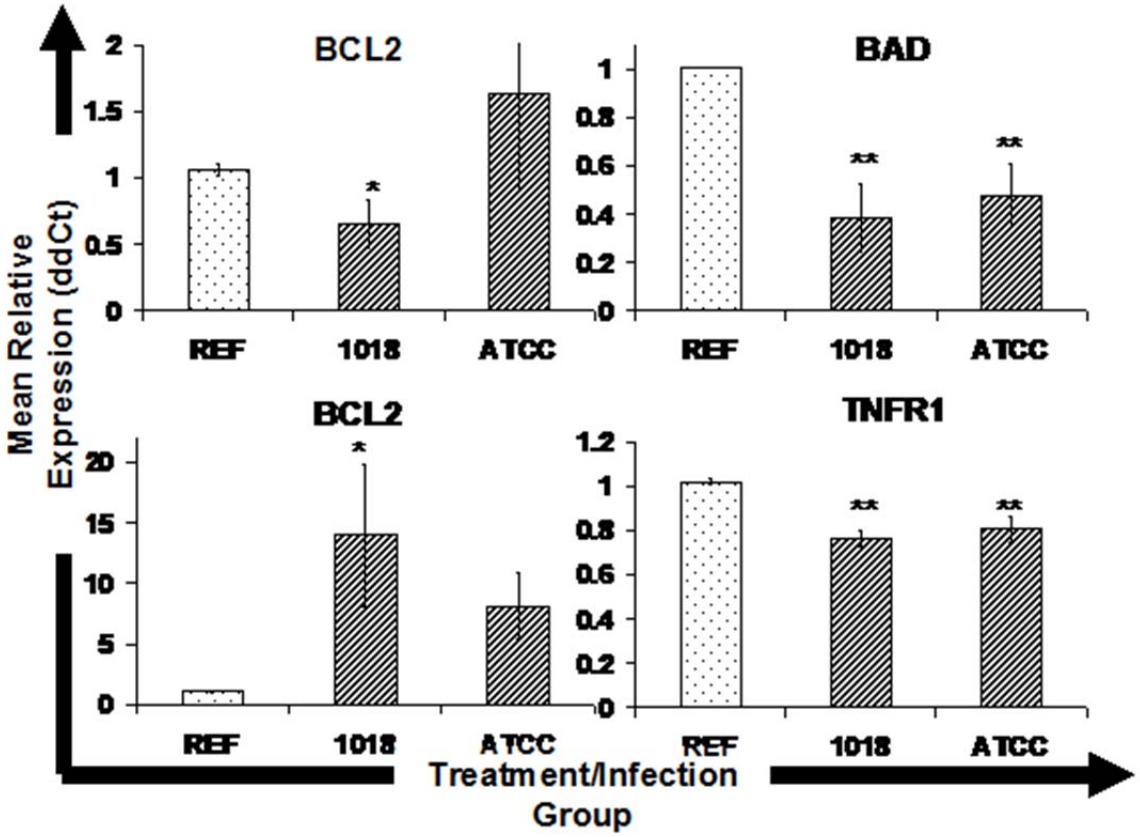

Figure 2.6-Expression of non-BOTL5 apoptosis genes in mature MDM cells following infection with MAP. Gene expression was assessed by Real Time qRT-PCR as previously described. Data was analyzed via the ddCt method using beta-actin as the control gene. The uninfected sample (REF) is indicated by the dotted sample while infected samples are shown with slashing lines. The bars represent the average results of MDM cultured from six animals. Error bars represent SE between the six biological replicates. * indicates significantly different from controls at a $p < 0.05$ and ** indicates significantly different from controls at $p < 0.01$.

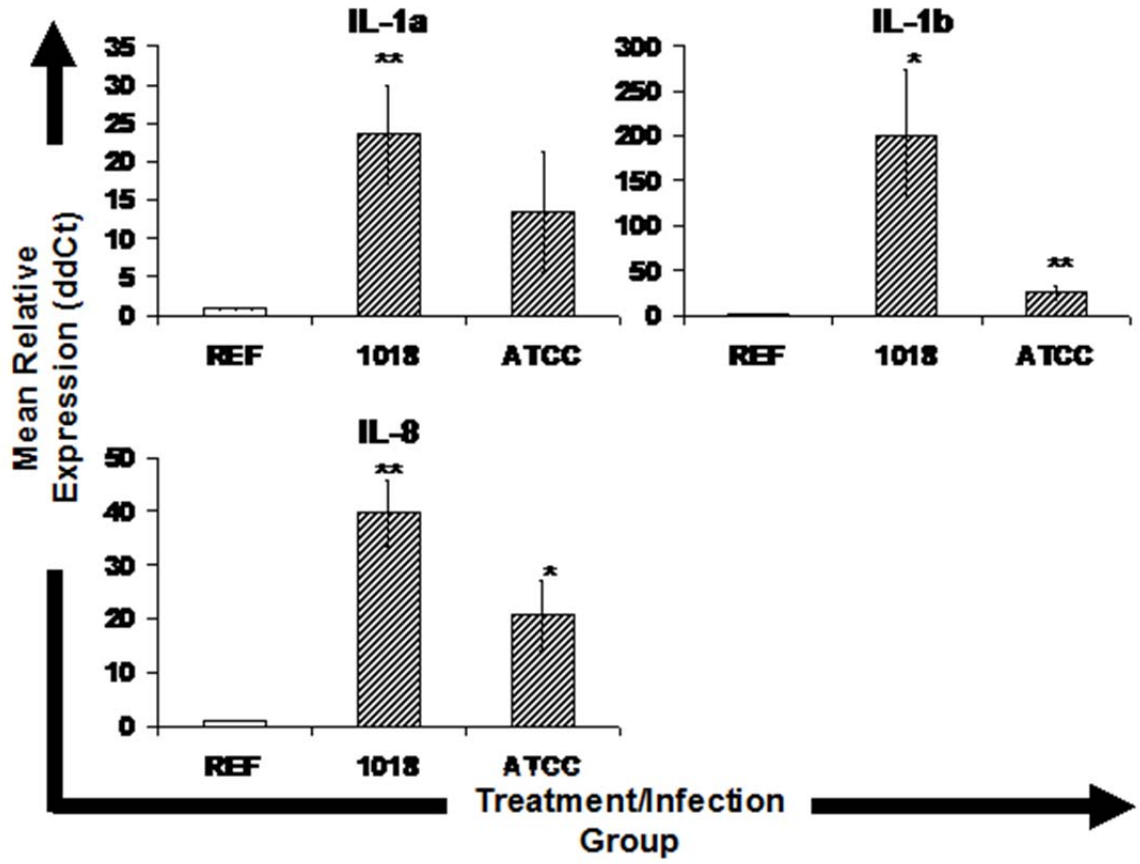

Figure 2.7-Expression of non-BOTL5 immune system genes in mature MDM cells following infection with MAP. Gene expression was assessed by Real Time qRT-PCR as previously described. Data was analyzed via the ddCt method using beta-actin as the control gene. The uninfected sample (REF) is indicated by the dotted sample while infected samples are shown with slashing lines. The bars represent the average results of MDM cultured from six animals. Error bars represent SE between the six biological replicates. * indicates significantly different from controls at a $p < 0.05$ and ** indicates significantly different from controls at $p < 0.01$.

Chapter 3

Rapid Identification of Sequences on a Microarray using Freely Available Resources

E. Kabara[1] and P.M. Coussens[2]. [1]Department of Biochemistry and [2]Center for Animal Functional Genomics, Department of Animal Science, Michigan State University, East Lansing, MI.

Abstract

The proper annotation of sequences used in microarray or genomics projects is critical to interpreting data that is generated. The challenge is when annotations are needed for data about organisms that have been sequenced but lack complete annotation information. Here, we present a method to quickly and accurately annotate sequences used in genomic studies using freely available and easily manipulated tools. Utilizing the method outlined below, we have reannotated our custom-made BOTL5 microarray and were able to annotate an additional 24% of the sequences found on the BOTL5 array. This resulted in annotations for over 87% of the microarray's sequences, which represent genes from *Bos Taurus*.

Introduction

While the number of projects using genomic data increases, so does the necessity for proper annotation of the sequences used in research. The main problem that these projects face is a lack of proper annotation of data for the species of interest due to the small amount of genome sequences available. While much is known about the genome and encoded proteins of *H. sapiens* or *A. thaliana*, comparatively little is known about the genomes of other animals and plants. If

researchers study these lesser-known species, they must properly annotate genes in the organism of interest, usually through homology to a better studied species. As more un-annotated organisms are studied more information about an organism of interest, such as similarity to other organisms and additional genomic sequences, will add to the previously reported results. Using the example of cattle, in the Gene Expression Omnibus there are over 3, 342 samples submitted for the period 2002 to 2011. While later samples do have significant annotations, a quick method to reannotate the earlier work may benefit original researchers by providing new insights into older studies. Reannotation may also facilitate meta-analyses across many microarray platforms. Here, we present a method to quickly and accurately annotate sequences used in genomic studies using freely available and easily manipulated tools.

Materials and Methods

Microarray DNA Sequences

Sequences of all spots on the BOTL5 microarray are available for download from the Center for Animal Genomics Website (http://www.cafg.msu.edu) as a single compressed FASTA data file. Sequences were downloaded in March 2011.

REFSEQ FASTA Sequence and GENEBANK Data

The known bovine, human, and Non-Redundant (NR) sequences were downloaded from the REFSEQ database (ftp://ftp.ncbi.nlm.nih.gov/refseq/).

Operation Environment

All computations were performed on a Windows 7 computer using 6 GB of RAM, a quad core 2.4 GHz processor, and 10 GB of hard drive space. For ease of use and installation of other components, the Cygwin Linux environment was installed (http://www.cygwin.com/).

Computation

For scripting and analysis, the language Python was installed into the Cygwin environment as part of the initial installation. The Basic Local Analysis Search Tool (BLAST) was used to compare sequences from each database to the microarray sequences. BLAST is freely available from http://blast.ncbi.nlm.nih.gov/Blast.cgi?CMD=Web&PAGE_TYPE=BlastDocs&DOC_TYPE=Download. Throughout the analysis, an E-value threshold of 10^{-10} was used to eliminate sequences from consideration. Only the most similar sequences were used to annotate a gene feature on the microarray.

For the human, bovine, and NR databases, the FASTA files were converted to a BLAST database. This step is required for the creation of a database of smaller seed sequences, which is necessary for a BLAST database search used to find an identical initial match for additional comparisons for query sequences. A more comprehensive explanation of the entire process can be found in Camacho et al.(2009)[69]. All three databases were downloaded and converted before any BLAST comparisons were performed. Formatting was performed by makeblastdb.exe using the command for a protein database:

```
./makeblastdb.exe -in FASTA_DATABASE
```

The command was changed when performed using a nucleotide database such as the bovine mRNA database:

```
./makeblastdb.exe -in FASTA_DATABASE -dbtype nucl
```

After the BLAST databases had been created, comparisons using the BLAST algorithm were performed to determine the similarity of two sequences. While an in-depth discussion of the BLAST analysis is beyond the scope of this publication, a full description of this algorithm can be found in Altschul et al.(1990)[70]. For our purposes, we wanted to find only the highest homology sequence in a database with an E-value cut-off of 10^{-10}. In addition, we also wanted to retrieve a tab-delimited file without comment lines for our output. However, since the BOTL5 and bovine mRNA sequences are nucleotide sequences and the human and NR databases are protein sequences, two different BLAST algorithms must be used. To compare a FASTA file of nucleotide sequences to a nucleotide database, this command was used:

```
./blastdn.exe -in FASTA_NUCLEOTIDE_SEQ -db NUCLEOTIDE_DATABASE -
outfmt 6 -max_target_seqs 1 -evalue 0.000000001 -out
BLAST_FORMATED_FILE_NAME
```

To compare a FASTA file of nucleotide sequences to a protein database, this command was used:

```
./blastdx.exe -in FASTA_NUCLEOTIDE_SEQ -db PROTEIN_DATABASE -outfmt
6 -max_target_seqs 1 -evalue 0.000000001 -out
BLAST_FORMATED_FILE_NAME
```

To compare a FASTA file of protein sequences to a protein database, this command was used:

./blastdp.exe -in FASTA_PROTEIN_SEQ -db PROTEIN_DATABASE -outfmt 6 -max_target_seqs 1 -evalue 0.000000001 -out BLAST_FORMATED_FILE_NAME

As the BLAST program produced tab-delimited files, a Python script file is provided for easy manipulation of the tab delimited files. The file performs three key tasks. First, it produces a FASTA file of the remaining un-annotated sequences after a BLAST comparison via remainder:

./python microarray_analysis.py remainder FASTA_MICROARRAY_FILE BLAST_ALIGNMENT_FILE OUTPUT_FILE

A second script consolidates 2 BLAST alignments or tab delimited files into a single file via consolidate:

./python microarray_analysis.py consolidate BLAST_TAB_FILE BLAST_TAB_FILE OUTPUT_FILE

A third script uses a second FASTA file and renames the known sequences to match the names of the original microarray sequence names via rename:

./python microarray_analysis.py rename BLAST_DB_FASTA BLAST_ALIGNMENT_FILE OUTPUT_FILE

Workflow

The expansion of the known bovine genome sequences and continued upgrades to the human and NR Refseq databases allowed for additional comparison between the bovine microarray and bovine mRNA, human protein, and NR protein databases. A diagram of the general workflow is presented in Figure 3.1. After a comparison of the human protein sequences with the BOTL5 microarray, several BOTL5 sequences did not have an annotation as determined by the `remainder` script. Therefore, we compared the BOTL5 sequence to the known bovine mRNA sequences. This step found whole bovine mRNA sequences rather than the partial cDNA sequences on the BOTL5 microarray. Based on the previous comparison, whole bovine mRNA sequences with high similarity to the BOTL5 sequences were renamed to match the BOTL5 sequence names via `rename`. These sequences were compared to the human protein database. Then, human sequences that displayed homology to the bovine mRNA sequences were considered to be the proper BOTL5 annotation. Alignments from the first and second round of BLAST annotation were then consolidated via `consolidate`. Finally, a FASTA file of unknown BOTL5 sequences was created via `remainder`. Additionally, BOTL5 sequences that did not exhibit homology to either the human or the bovine databases were compared to the NR database using the same strategy and programs above. The NR database allowed for sequences not found in either the human or bovine database to be compared to the BOTL5 sequences. Similar to the bovine mRNA process, the NR protein sequences with high homology to BOTL5 sequences were compared to the human protein database.

Results and Discussion

By adding intermediary steps to the BLAST annotation of a microarray, we were able to successfully annotate 87% of the BOTL5 microarray (Figure 3.2). This is a major improvement

over the previous simple annotation of the BOTL5 microarray, which used only known human proteins. By adding the bovine mRNA database, we added 23% more known sequences to the microarray annotation files. Finally, the use of the NR protein database added a small yet significant number of sequence annotations. NR additions amount to approximately 1% of the total sequences while accounting for almost half of the total time commitment of this project. However, 13% of the sequences are still unknown. The BOTL5 microarray was created from mRNA isolated from bovine leucocytes that were further amplified in bacteria. Because of this, we expected a portion of the microarray to lack any significant annotation to mammalian sequences due to the shortage of sequence isolation or because of outside sequence contamination[71].

The use of an mRNA or cDNA database was a major improvement over a simple BLAST against a more commonly studied species. As this example demonstrates, an additional 23% of the BOTL5 microarray was annotated using this process. The annotation of additional sequences can be attributed in part to the inclusion of 5' and 3' UTR regions as well as splice isoforms found in an mRNA database specific to the particular organism of interest. If some of our microarray sequences were from one of the non-translated areas that are not part of a protein database, then no sequence homology would be found in the human protein database. However, by using an intermediary sequence from the mRNA database to find proteins in a protein database, homology to a larger sequence could be found. Increased homology allows for the original sequence on the microarray to be successfully annotated.

The use of the NR database for this work may be a concern to some researchers. As reported before, a BLAST comparison of the NR database with approximately 200 BOTL5 microarray sequences took over 10 hours to complete. But, this step only resulted in 12

homologous sequences. Similar searches against just the human or bovine mRNA databases took approximately 2 hours. While NR comparisons will find homologous sequences, a simple annotation using only the human protein and bovine mRNA databases would provide a relatively high degree of annotation to the microarray. A possible alternative may be to use other sequence databases, such as the vertebrate protein database, for the final sequence comparison.

While this method allowed for additional annotation of the BOTL5 microarray, it does have a significant problem. Any additional annotations to a sequence set are dependent on the known information of the bovine and human genome and proteome. BLAST is an excellent method for exclusion of obvious contamination from analysis. However, sequences that display homology to the bovine genome and do not present homology to any bovine or human protein will not be able to be annotated. Sequences from stretches of the genome that are transcribed but not translated such as rRNA will not find any similarity within the human or NR protein databases. Untranslated sequences are important, therefore other methods of study must be implemented to determine homology for these sequences.

As a final note, reannotation of a microarray should be performed on a regular basis to determine the most up to date annotation. The NCBI releases regular monthly updates to their annotation and FASTA files. Although, most of the monthly update changes were relatively unnoticeable, some can be quite drastic. The addition of a small number of sequences to a family of proteins significantly changed the outcome of several of our experiments. Therefore, while we do not advocate daily updates of any microarray annotations, a monthly reannotation or update at the start of a major project is worthwhile. With the quick and economical nature of this process, we feel other researchers should consider reannotating previously published microarray data as novel annotations may provide original insights into previously reported results.

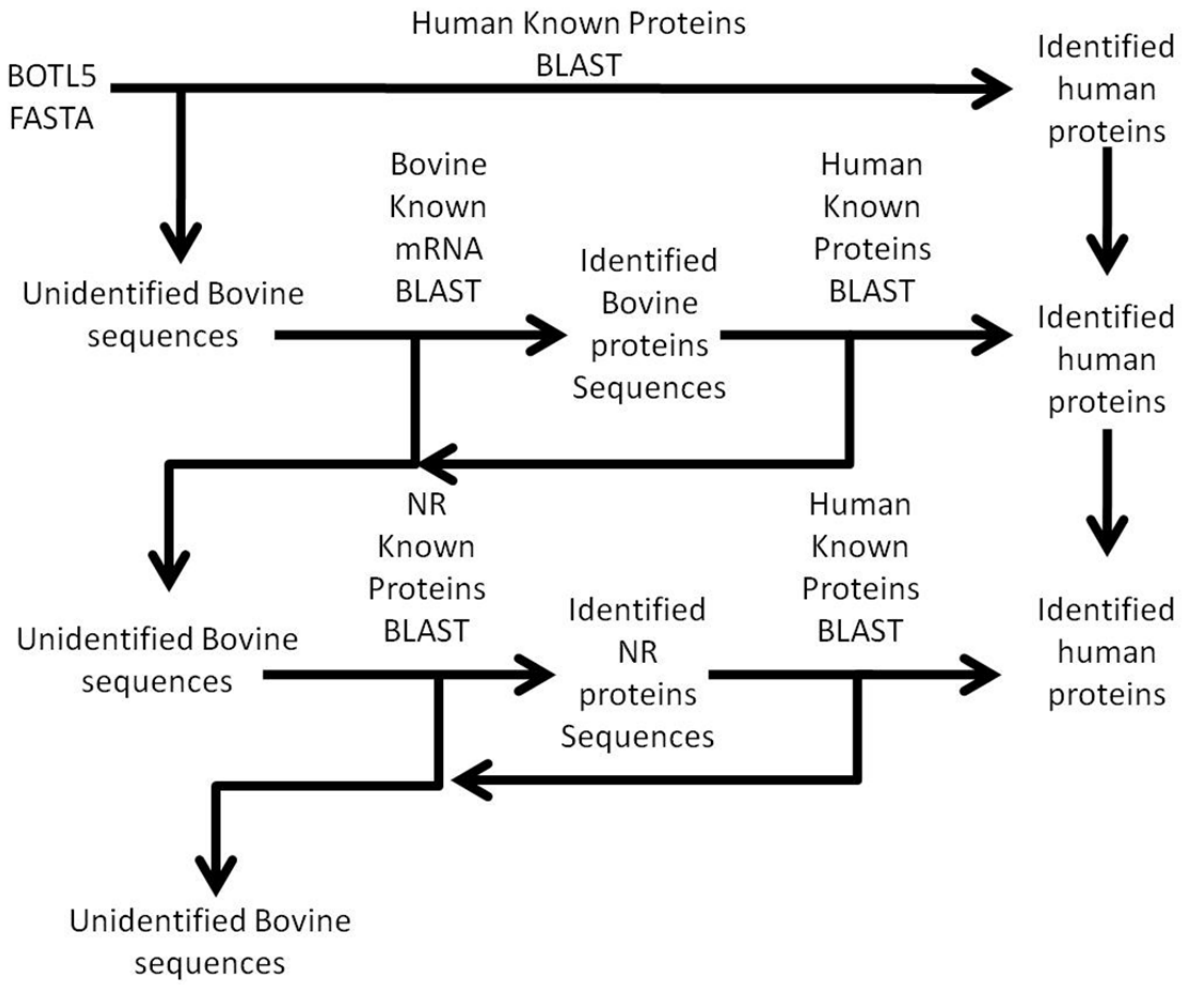

Figure 3.1: Sequence Annotation Work Flow Diagram Above is the general work flow for the reannotation of the BOTL5 microarray. First, BLAST was used to annotate sequences that displayed high homology to human sequences. This first pass annotated the largest number of sequences. Next, sequences that did not posses high homology to humans were compared to bovine known protein sequences via BLAST. Instead of using the sequences from the microarray, the bovine protein sequences that corresponded to the similar yet unknown microarray sequences were then compared to the human protein database again via BLAST. Sequences that did not exhibit high homology via the previous comparison were then compared to the Non-Redundant (NR) protein database to find protein sequences of high similarity in any

research organism. Full-length sequences from the NR database with high homology to the BOTL5 sequences were then compared to BLAST a final time to retrieve any missing human annotations.

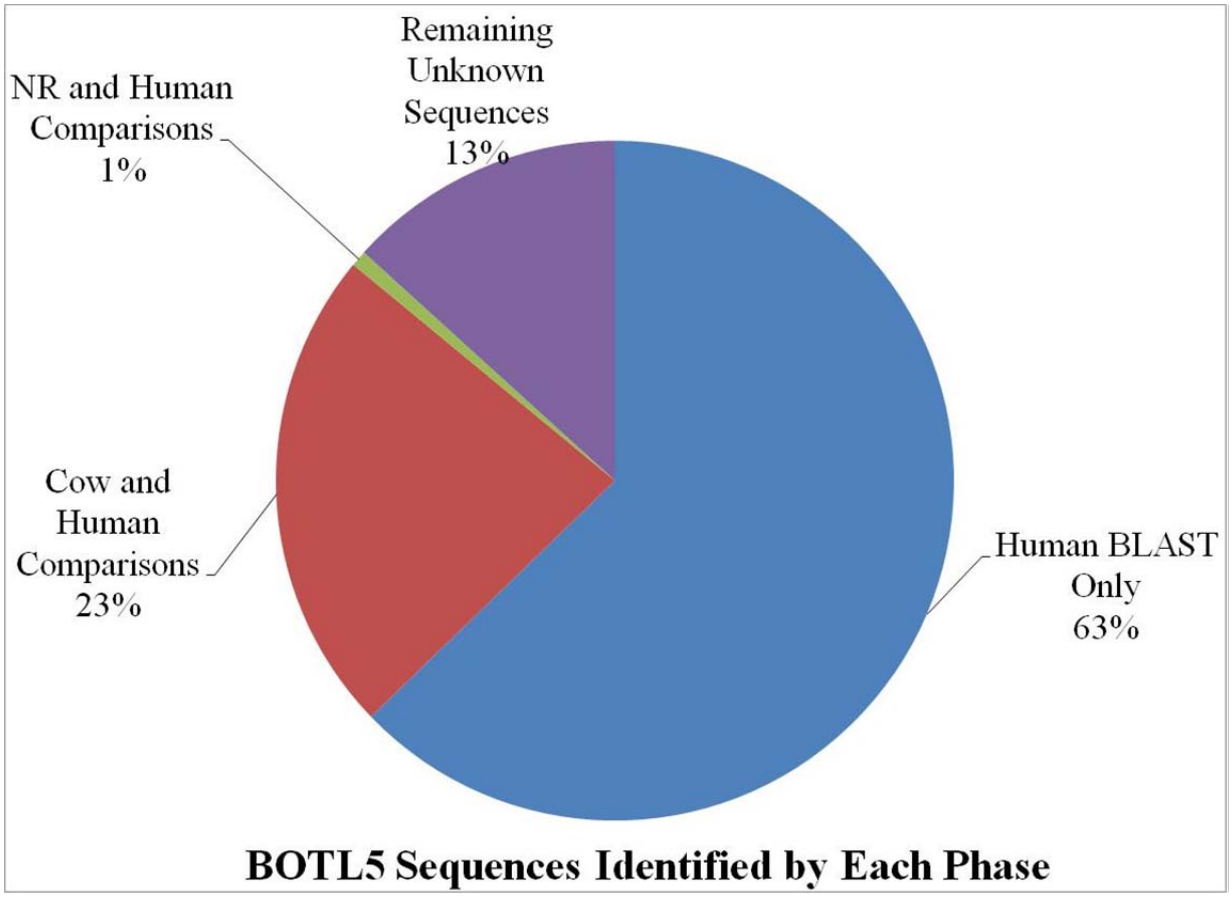

Figure 3.2 BOTL5 Sequences Identified by Each Stage Each section of the pie chart represents the percentage of BOTL5 sequences found in each part of annotation procedure. The largest percentage of sequences was annotated by a simple comparison to the human protein database. Next largest group was BOTL5 sequences that were based on similarity to cattle mRNA sequences and a comparison to the human protein sequences. The smallest portion of the microarray annotated was the remaining BOTL5 sequences that were compared to NR database sequences. After the entire procedure, less than 13% of the microarray remained unannotated.

Chapter 4

Infection of primary bovine macrophages with *Mycobacterium avium* subspecies *paratuberculosis* suppresses host cell apoptosis.

E. Kabara[1] and P.M. Coussens[2]. [1]Department of Biochemistry and [2]Center for Animal Functional Genomics, Department of Animal Science, Michigan State University, East Lansing, MI.

Abstract

Mycobacterium avium subspecies *paratuberculosis* (MAP) is one of the most important infectious agents in the American dairy industry. MAP is able to survive intracellularly in macrophages by preventing normal phagosome maturation processes utilized to destroy bacteria. Macrophages often undergo apoptotic cell death in response to intracellular pathogens. This allows for the efficient presentation of bacterial antigens to the hosts adaptive immune system in a process known as efferocytosis. Recent studies with *Mycobacterium tuberculosis* (MTB), a mycobacterium related to MAP, showed that macrophages infected with MTB are less likely to undergo apoptosis than control, uninfected cells. It is proposed that regulation of macrophage apoptosis is an important immune evasion tactic for MTB. Based on the similarity of MAP and MTB, we hypothesize that MAP infected macrophages will be resistant to apoptosis compared to uninfected cells within the same culture and to cells from uninfected cultures. Our results demonstrate that populations of MAP-infected macrophages contain fewer apoptotic cells than similar populations of control cells, and that MAP-infection reduces the sensitivity of infected macrophages to induction of apoptosis by H_2O_2. We further demonstrate that MAP-infected cells contain reduced caspase activity than uninfected cells. Reduced caspase activity in MAP-

infected macrophages is also maintained after strong H_2O_2 stimulation. This reduction in activity is accompanied by a pronounced reduction in transcription of caspase genes when compared to control, uninfected cells. Furthermore, MAP-infection drastically effects the expression of several host cell proteins important for regulation of apoptosis. Studies using mutant MAP strains demonstrate the importance of several bacterial specific factors in the control of host macrophage apoptosis. Together these data demonstrate that MAP specific factors may prevent caspase gene transcription and apoptosis signaling protein expression resulting in decreased spontaneous host cell apoptosis and decreased sensitivity to apoptosis inducing agents.

Introduction

Mycobacterium avium subspecies *paratuberculosis* (MAP), the causative agent of Johne's disease, is found in over 68% of cattle herds in the United States. The largest percentage of these animals are subclinically infected with the bacterium [1]. Johne's disease costs the U.S. dairy industry up to $1.5 billion per year in loses [2]. A controversial but developing link between MAP and some cases of human Crohn's disease suggests that MAP may become a significant food safety concern [13].

One of the key factors that makes MAP such an elusive pathogen is its ability to survive inside host macrophages. Typically, macrophages phagocytose and destroy infectious pathogens. MAP, however, is able to prevent normal phagosome maturation allowing the bacteria to survive in stalled phagosomes, which become reservoirs for further bacterial growth [14, 72]. To better understand the nature of the host-pathogen interaction in infected macrophages, our group performed a large-scale microarray experiment to study the changes in

relative expression of hundreds of host genes in MAP infected cells. From the genes and pathways found to have altered expression, it was apparent that host cell apoptosis was an important area of focus [73].

Regulation of cell death is extremely important for proper defense against bacteria as well as other intracellular threats to the host. Intracellular bacterial or viral infections should lead to apoptosis of the infected cell to properly destroy the invading pathogen. The apoptotic control of infected cells is a highly conserved mechanism shared by members of both plant and animal kingdoms [74, 75]. After apoptosis of the infected cell, macrophages and other cells then phagocytize the remaining cellular debris and apoptotic blebs containing pathogens, a process called efferocytosis. Efferocytosis then leads to further immune stimulation and clearance of the pathogen from the host. Defects in efferocytosis lead to disease progression in *F. novicida* and *Y. enterocolitica*, infections as well as in arteriosclerosis [76-78]. Conversely, if the infected cell dies by necrosis, pathogens will be released and allowed to spread to new targets [45, 79, 80].

Cell death has recently been a focus of studies in mycobacteria other than paratuberculosis, particularly with the human pathogens *Mycobacterium tuberculosis* (MTB) and *Mycobacteria leprae* (ML). MTB can induce apoptosis in heavily infected cells, however, it is now clear that MTB actually suppresses early apoptosis of infected cells as a way for the bacteria to survive intracellularly [45, 79, 81-83]. ML, in contrast, causes necrosis of infected cells, releasing the bacteria to infect other cells in the host [84].

Recently, Kelly et al. demonstrated that MTB-infected cells induce apoptosis in bystander cells through a cell contact mechanism. The phenomenon described in Kelly et al. is referred to as “the bystander effect” [37]. These results suggest that when infection rates are low to moderate, studies using whole culture lysates for techniques such as western blotting,

microarrays, and PCR may result in data that does not account for interactions between infected cells and uninfected cells (bystander cells) within the same culture.

The focus of our current study was to understand how MAP may affect apoptosis pathways in bystander and MAP-infected macrophages. We provide evidence that MAP-infected macrophages are less likely to undergo apoptosis than either bystander or uninfected macrophage controls with and without induction by H_2O_2. Apoptotic signal transduction in MAP-infected macrophages was also examined. MAP-infected macrophage cultures contained a lower percentage of cells with high caspase activity when compared to bystander and control macrophages, even with strong apoptotic induction. We also observed a reduced abundance of mRNAs encoding several host cell caspases in MAP infected macrophages. While there were no apparent differences in activation of mitogen activated protein kinase (MAPK) pathway members, we did observe distinct differences in abundance of several key host proteins involved in regulation of apoptosis. Finally, we studied apoptosis of macrophages infected with several MAP mutants to determine if MAP specific factors may be involved in regulation of host cell apoptosis. Our novel results suggest that indeed, MAP genetic elements play a role in preventing apoptosis of infected cells.

Materials and methods

Experimental Animals

Uninfected, healthy Holstein cattle at the Michigan State University Dairy Teaching and Research Center were selected as a source of monocyte derived macrophages (MDM cells) for this study. Cattle were tested for MAP via the IFN-γ test (Bovigam, Biocore Animal Health, Omaha, NE), fecal culture, and ELISA tests (Michigan State University Diagnostic Center for

Animal and Population Health, East Lansing, MI). All animal handling procedures were approved by the Michigan State University Committee on Animal Use and Care.

Cell Culture

Isolation of peripheral blood mononuclear cells (PBMC)s was performed using 1x Ammonium Chloride lysing solution on buffy coats extracted from whole blood after centrifugation. PBMC were plated in 150 cm^2 flasks at 1.0-1.5x10^8 per flask and washed with 1x PBS after 24 hours to remove non-adherent cells. At three days post plating, monocyte-derived macrophages (MDM) were harvested using 0.25% Trypsin as suggested by the manufacturer (Invitrogen, Carlsbad, CA). MDM were then replated in RPMI 1640 media to obtain the necessary number of cells needed for each experiment.

Bacterial Culture

Mycobacterium avium subspecies *paratuberculosis* (MAP) strain #19698 was previously purchased from the American Type Culture Collection (ATCC, Manassas, VA) and MAP strain SS149 was generously provided by Dr. Sri Sreevatsan (University of Minnesota, Minneapolis, MN). Both MAP strains were grown at 37^{o}C in Middlebrook 7H9 media (Difco Laboratories, Detroit, MI) supplemented with 2mg/ml Mycobactin J (Allied Monitor, Lexana, KS) and 10% Middlebrook OADC enrichment (BD Biosciences, Sparks, MD). MAP cultures were grown for four months prior to harvesting bacteria for infections. Concentration of MAP was determined via serial dilution and counting on a bacterial hemocytometer. Bacteria were stored at 4^{o}C prior to infection of MDM cells. Periodic acid-fast tests were performed to check each culture was a pure mycobacteria culture.

Bacterial staining and infection protocol

MAP cultures were vortexed for 1 minute to disrupt clumps prior to use. Based on the initial bacterial concentration, a premeasured volume of bacterial culture was placed in a 1.5ml eppendorf tube. An equal volume of 1,1'-dilinoleyl-3,3,3',3'-tetramethylindocarbocyanine perchlorate (DiI) (Invitrogen, Carlsbad, CA) was added and the bacteria/staining solution was vortexed and placed in a dark area for 30 minutes. After this time, the stained bacteria were centrifuged at 13,000 X G for five minutes and washed three times with 1ml 1x PBS. Post washing, labeled bacteria were suspended in PBS. A volume of the labeled bacteria solution was added to each MDM-MAP infection plate such that the total amount of labeled bacteria would be 20 times the amount of MDM present in each sample (MOI=20). MAP-infected cultures were washed with 1x PBS at 24 hours post infection to remove all non-phagocytosed bacteria.

Apoptosis Labeling

MDM cells were harvested in 1x Annexin V binding buffer (BD Biosciences, Franklin lakes, NJ). Annexin V-FITC and 7-AAD were then added to the cell suspension. This cell suspension was then placed in a dark area at room temperature for 15 minutes. Post labeling, 1x binding buffer was added to the cell solution to quench the staining reaction. Stained cells were then analyzed using a BD FACSCalibur flow cytometer. Cells were electronically gated based on size and granularity to remove debris from final analyses. Cells were then separated into infected and bystander populations, based on fluorescence (or lack of fluorescence) from the DiI labeled MAP. After initial gating, cells were divided into one of three groups: pro-survival, apoptotic, and necrotic. Cells that showed low staining for both Annexin V and 7-AAD were

considered pro-survival cells. Cells that show low Annexin V staining, but stain with 7-AAD are considered necrotic cells. Cells with high Annexin-V staining regardless of 7-AAD status are considered apoptotic cells.

Caspase Activity Assays

MDM cells were labeled using the CaspaTag system for monitoring activity of caspases 3/7, 8, and 9, essentially as recommended by the manufacture (Millipore, Billerica, MA). This label binds to the active form of each of target caspases. Caspase activity was analyzed using a BD FACSCalibur flow cytometer. As before, cells were initially gated based on size and granularity, then by MAP infection status. Cells within these groups were further divided into two additional groups: those cells showing low caspase activity and those cells showing high caspase activity. All cells contain some caspase activity and this methodology is a standard way of distinguishing apoptotic cells (high caspase activity) from non-apoptotic cells (low caspase activity). To test the division of cells into these two groups based on caspase activity, cells were treated with hydrogen peroxide (H_2O_2), which is known to stimulate caspase activity. We observed a clear shift of cells moving from the low caspase activity group to the high caspase activity group, confirming the use of these categories.

Antibody Labeling

MDM were harvested in 1x Fixation/Permeabilization buffer (eBioscience, San Diego, CA) prior to intracellular labeling. MDM were labeled using antibodies specific to several host proteins involved in the MAPK pathway or in apoptosis (TABLE 4.1). Antibody labeling occurred while in 1x Fixation/Permeabilization buffer and all cells were washed using 1x Fixation wash

solution. Antibody labeled MDMs were diluted in 300 µL of 1x PBS. Protein concentration and phosphorylation was evaluated in labeled cells using a BD FACSCalibur flow cytometer as per the manufacturer's instructions.

Quantitative real time reverse transcriptase PCR (RT-qPCR)

Control, uninfected MDM or MDM cells infected with MAP strain SS149 at a MOI 20:1 were lysed and processed to obtain total RNA using the 5 Prime RNA extraction kit as suggested by the manufacturer (5 Prime, Gaithersburg, MD). Real Time qRT-PCR primer design, cDNA synthesis, PCR methods, and data analysis were performed as previously described [73]. A full list of primers and sequences are available on the Center for Animal Functional Genomics website (http:/www.cafg.msu.edu).

Results

Spontaneous apoptosis in MAP-infected MDM cells

There were significant differences in the percentage of cells undergoing spontaneous apoptosis between populations of MAP-infected, bystander, and control macrophages. MAP-infected macrophages had a significantly lower relative percentage of apoptotic cells when compared to both bystander and control macrophages ($p=0.0098$ and 0.0056, respectively) (Figure 4.1A). Populations of bystander macrophages tended to contain a higher percentage of apoptotic cells than control cells from uninfected cultures ($p=0.08$). No significant differences were apparent when the relative percentage of necrotic cells was examined in the three populations (data not shown). As expected, populations of MAP-infected macrophages showed a larger percentage of pro-survival cells when compared to bystander and control cells ($p=0.0098$

and 0.0056, respectively) (Figure 4.1B). Bystander cell populations displayed fewer pro-survival macrophages than control cells (p=0.0424). This leads us to conclude that MAP-infected macrophages are less likely to spontaneously enter apoptosis than cells from control, uninfected cultures. Conversely, bystander cells are more likely to enter apoptosis than cells from control, uninfected cultures.

MAP-infected macrophages are more resistant to induction of apoptosis then control or bystander macrophages

Based on differences in spontaneous apoptosis observed between MAP-infected, bystander, and control cell populations, we studied the relative resistance of these three cell groups to induction of apoptosis. Hydrogen peroxide (H_2O_2) is a well-known apoptotic inducing agent [85]. We chose to use 100uM H_2O_2 for 20 minutes, based on time course and dose-response curve studies with uninfected MDM (data not shown). All cell populations exposed to H_2O_2 displayed a higher percentage of apoptotic macrophages than their untreated sister cultures ($p< 0.05$). When H_2O_2-treated macrophages were compared across the infection groups, H_2O_2-treated MAP-infected MDM cell populations contained a significantly lower relative percentage of apoptotic cells than either bystander or control macrophage populations (p=0.0448 and 0.0278, respectively) (Figure 3.2). No significant differences were observed in the percentage of necrotic cells between the three infection groups (data not shown). H_2O_2-treated bystander macrophage populations were not significantly different then H_2O_2-treated control macrophage populations.

MAP-infected macrophages have much less caspase activity then control or bystander macrophages

MAP-infected macrophage populations had a lower percentage of spontaneously apoptotic cells than control or bystander macrophage populations. MAP-infected macrophages also showed a higher resistance to H_2O_2 driven apoptosis induction. Given the importance of caspases in apoptosis, we determined if MAP infection had an effect on caspase activity. We focused on monitoring activity for caspases 3/7, 8, and 9. Because H_2O_2 efficiently induced apoptosis in all cell types, we chose this reagent to induce the cells during caspase studies.

Caspases 3/7, 8, and 9 all showed very similar patterns of activity in untreated cells. Uninfected, control macrophage cultures contained the highest relative percent of cells with high caspase activity. Bystander macrophage populations contained an intermediate percentage of cells with high caspase activity. MAP-infected macrophage populations contained the lowest percentage of cells with high caspase activity. Regardless of the caspase studied, all three of these groups were significantly different from one another ($p< 0.05$) (Figure 4.2A).

As before, cells were exposed to 100uM H_2O_2 for 20 minutes to induce apoptosis. The relative percentage of cells with high caspase activity in control, bystander, and MAP-infected MDM populations was significantly higher following H_2O_2 induction compared to populations from untreated sister cultures, regardless of the caspase studied ($p< 0.05$). MAP-infected macrophage populations contained a significantly lower relative percentage of cells with high caspase activity than either control or bystander MDM populations for caspases 3/7, 8, and 9 ($p< 0.05$). However, no significant differences were observed between control and bystander macrophage populations for any of the caspases studied (Figure 4.2B).

MAP-infection reduces caspase mRNA abundance

Based on our finding that MAP-infected cell populations had generally lower caspase activity, we next focused on caspase mRNA abundance. We studied the relative abundance of mRNA encoding caspases 3, 7, 8, and 9. Differences in caspase gene expression or mRNA abundance could explain the observed reduction in caspase activity in MAP-infected macrophages. For this work, we used the bovine isolated MAP strain SS149. SS149 routinely infected over 85% of cells in a culture at a MOI of 20. We infected MDM with DiI-labeled SS149 and determined the percentage of macrophages that were infected in each culture using flow cytometry. We considered macrophages cultures infected with MAP at or over 85% to be heavily infected and thus suitable for whole culture analyses. We observed significantly less mRNA encoding caspases 3, 7, and 8 in macrophages infected with MAP SS149 than in control, uninfected macrophages ($p<0.05$). However, no significant differences were observed for mRNA encoding caspase 9 (Figure 4.5). Thus, reduced expression of caspase mRNA in MAP-infected macrophage cultures could, at least partially, explain the observed reduction in caspase 3/7 and 8 activity. However, other factors would need to be considered to explain the observed reduction in caspase 9 activity.

MAP-infected and control macrophages have distinct differences in apoptotic protein expression.

As caspase 9 mRNA levels were not altered in macrophage cultures following MAP infection, we sought other mechanisms to account for observed differences in caspase 9 activity in MAP-infected cells. Work from other groups suggested that host gene or protein expression of BAD, AKT, and MCL-1 displayed significant differences in control cultures and macrophage cultures infected with either MAP, ML or MTB [73, 86, 87]. To determine if MAP-infected macrophages showed differences in protein expression in our system, MDM were infected with

MAP SS149 for 24-hours and treated with either M-CSF to stimulate production/activation of BAD and AKT or GM-CSF to stimulate activation of MCL-1. After M-CSF treatment, control uninfected MDM exhibited significantly more unphosphorylated and phosphorylated BAD than untreated cells. M-CSF treatment of MDM previously infected with MAP SS149 also enhanced levels of unphosphorylated and phosphorylated BAD, but not to the extent observed in uninfected cells (Figure 4.5). A similar reduction in the phosphorylation of AKT was also observed in MAP-infected cultures as compared to uninfected cultures (Figure 4.5). In each case observed differences were significant ($p < 0.05$). MAP-infected MDM treated with GM-CSF demonstrated significantly lower expression of MCL-1 when compared to control uninfected cultures also treated with GM-CSF ($p< 0.05$) (Figure 4.5). In each case, there were also significantly fewer cells positive for the various proteins in MAP-infected MDM cultures than in control uninfected cultures ($p<0.05$).

Mutant MAP strains fail to control host cell apoptosis

As we examined the host response to MAP, we were also interested in what MAP factors might be involved in regulating host cell apoptosis. To examine the role that specific genes play and identify areas of the MAP genome involved in alteration of macrophage apoptosis, several mutant MAP strains were obtained from the Johne's Disease Integrated Program (JDIP) in a blind study. For this work, we were only interested in the relative percent of cells undergoing spontaneous apoptosis following MAP infection, compared to control uninfected cells, thus data from bystander macrophages is not shown. In Figure 4.6, the percentage of spontaneous apoptotic cells is shown for control (uninfected), ATCC 19698-infected (wild-type), and several strains of mutant MAP-infected macrophages. As before,

ATCC 19698-infected macrophage cultures contain a lower relative percentage of apoptotic cells than control, uninfected cultures ($p < 0.05$). One MAP mutant (204) appeared to also significantly reduce macrophage apoptosis whereas most others did not. Two mutants (221 and 222) actually enhanced apoptosis in infected cultures, relative to control uninfected cultures ($p<0.05$). Details on the individual strains used as well as the mutant gene in each of these MAP strains is shown in TABLE 4.2. Our data indicates that MAP1719c and MAP1872c mutated in strains 221 and 222, respectively, are likely important for MAP-infection driven regulation of host cell death.

Discussion

Apoptosis of infected cells is an important immune control tactic in defense against intracellular pathogens [45, 79, 80]. However, some pathogens may prevent host cell apoptosis, circumventing efferocytosis, and ensuring limited immune system detection [88]. A report by Kelly et al showed control of host cell apoptosis exerted by MTB in both infected and bystander cells (uninfected cells in an infected culture) [37]. While this report clarified the regulation of apoptosis in MTB-infected macrophages, comparatively little is known about how MAP might regulate apoptosis in Johne's disease. In this study we sought to determine if MAP altered host cell apoptosis, to investigate the bystander effect during MAP infection, and to begin examining bacterial factors that may control apoptosis in MAP-infected macrophages. Our results clearly demonstrate that MAP-infected macrophage cultures contain a higher percentage of pro-survival cells when compared to bystander and control cell populations. Thus, our results with MAP suggest a similar control over host cell apoptosis as described for MTB [37]. Unlike MTB, however, we did not observe a significantly enhanced level of apoptosis in bystander cell populations compared to control, uninfected cultures.

As apoptosis is heavily regulated in the host, we next wanted to study how MAP-infected, bystander, and control cells reacted to induction of apoptosis by an exogenous agent. MAP-infected macrophages were significantly less sensitive to induction of apoptosis by H_2O_2 when compared to both control and bystander cells (Figure 4.2). This data demonstrates that MAP infection reduces the ability of only MAP-infected macrophages to enter apoptosis as no protection was extended to bystander macrophages in an infected culture. This indicates that the MAP-infection driven mechanism of macrophage survival likely relies on the presence of bacteria within the cell.

Since MAP-infected macrophages are less likely to undergo apoptosis than control or bystander macrophages, any efforts by the host to induce apoptosis specifically in MAP-infected macrophages would most likely induce apoptosis in surrounding cells and tissues, while leaving the intracellular bacteria relatively unscathed. An important consequence of a lower relative percentage of apoptotic cells in MAP-infected macrophages would be lack of efferocytosis. Therefore, less MAP antigen presentation to the innate immune system that could have a deleterious effect on development of a proper immune response.

As infection with MAP resulted in clear control of spontaneous and induced apoptosis in macrophages, our next goal was to begin establishing the host pathways altered in infected cells that might explain inhibition of host cell death. To elucidate the pathways involved, we studied the caspase activity of cells under different infection conditions. MAP-infected macrophage populations had the lowest percentage cells with high caspase activity, even with strong apoptotic induction by H_2O_2 (Figure 4.3). Since caspases are central to apoptotic pathways, we conclude that this block may be an important part of MAP-mediated regulation of host cell apoptosis. A reduction in caspase activity could readily explain the significant differences in

apoptosis observed in our study, as less caspase would be available to signal within MAP infected cells. Our results with H_2O_2 demonstrated that, although there was an increase in caspase activity following treatment in the infected macrophage population, this was significantly less pronounced than in either uninfected control cultures or in the bystander cell population. These data suggest that infection of cells with MAP blocks the apoptosis pathway at a point upstream of caspase activation.

Danelishvili et al studied the role MTB plays in host caspase activity [89]. Two MTB proteins Rv3654c and Rv3655c were identified that bound host proteins involved in transcriptional regulation of caspases. They demonstrated increased caspase 8 activity in macrophages infected with an MTB Rv3654c mutant when compared to wild type MTB. While Rv3654c does not have a homolog in MAP, sequences exist that may be homologous to Rv3655c (444491-444262 in the MAP genome; E-value < 10^{-20}). Based on our caspase activation data, the results of Danelishvili et al, and the homology between MAP and MTB, we studied the relative abundance of several caspase mRNAs in MAP-infected macrophages. By selecting only cultures with little to no bystander macrophages present, we were able to marginalize the effect bystander cells would have on the results of a whole culture based analysis, such as RT-qPCR. We demonstrated that MAP infection reduces the mRNA abundance for genes encoding caspase 3, caspase 7, and caspase 8 when compared to uninfected controls (Figure 4.5). If reduction of caspase 3, caspase 7, and caspase 8 mRNA abundance manifest as a reduction in caspase 3, caspase 7, and caspase 8 protein, then less caspase would be available to signal in the cells offering a possible explanation for reduced caspase 3/7 and caspase 8 activity. However, because we observed no similar reduction in caspase 9 mRNA abundance this explanation does not appear to extend to a reduction in caspase 9 activity in infected macrophages.

In addition to our work studying the caspase and apoptosis cascade in MAP infected cells, we also studied other pathways that may be altered by MAP infection and that may account for the observed loss of caspase 9 activity. We found significantly lower expression of BAD, phosphorylated BAD (p-BAD), phosphorylated AKT (p-AKT), and MCL-1 in MAP-infected cultures relative to control, uninfected cultures (Figure 4.5). AKT phosphorylation is an important step in preventing apoptosis and reduced levels of p-BAD would also tend to favor apoptosis [90]. Thus, reduced p-BAD and reduced p-AKT could both lead to a reduction in overall apoptotic potential in cells. Reduced levels of MCL-1, a well known anti-apoptosis signaling protein, would tend to favor apoptosis in MAP-infected macrophages [91]. However, this effect is obviously offset by some other, perhaps as yet unknown, balance within MAP-infected macrophages. Signals from BAD, AKT, and MCL-1 eventually converge at the mitochondria, which is extremely important in regulation of apoptosis in MTB infected cells [92-94]. It is possible that pro-apoptotic signals (i.e. reduced MCL-1) may be present upstream of the mitochondria, but MAP prevents loss of mitochondrial membrane integrity. This in turn would prevent cytochrome C release and apoptotic signal transduction via caspase 9. Further work must be done to clarify the proteins and/or pathways involved in MAP induced changes in regulation of host cell apoptosis via caspase 9.

In addition to the aforementioned proteins, our group also studied the expression of several other host proteins in MAP-infected macrophages. MAPK signal transduction was previously studied by our group, but we did not specifically study the MAP-infected, bystander, and control macrophages during our initial work [95]. However, consistent with our previous results [95], we observed no significant differences in protein expression or activation within this group of proteins (p38, ERK1/2, and Jun/SAPK). Furthermore, we examined expression of

several other apoptosis signaling proteins, including TRADD, FADD, and FLIP in MAP-infected and control cells. Again, we observed no significant differences between expression of these proteins in MAP-infected and control cells.

Bystander macrophage populations tend to have a higher percentage of apoptotic cells than uninfected control cell cultures. However, we observed significantly fewer cells with high caspase activity in bystander cell populations when compared to control, uninfected cells. When bystander macrophage populations were treated with H_2O_2, no differences were observed between the control or bystander macrophages in terms of apoptosis or caspase activity. These data suggest that caspase signaling systems in bystander cells are reduced relative to those in control uninfected cells, but these systems can be induced to initiate apoptosis following induction by external stimuli. Mycobacteria are known to secrete several proteins and lipids into culture media, as well as exchange lipids with infected macrophages [89, 92, 96, 97]. Based on this information, bystander macrophages in MAP-infected cultures may be exposed to low levels of mycobacterial products that reduce caspase activity, but do not disable the system as in the infected cells.

Finally, we studied apoptosis in macrophages infected with several MAP mutants and compared the relative percentage of apoptotic host macrophages that found in uninfected control cultures and to populations of cells infected with MAP strain ATCC #19698 (Figure 4.6). Host macrophage populations infected with MAP mutant strains 222 or 221 contain a higher percentage of apoptotic cells compared to populations of uninfected control cells or populations of cells infected with ATCC #19698. The sequences mutated in MAP 221 (MAP1719c) encode a hypothetical protein sequence and with no function known at this time. MAP 222 contains a mutation in the mbth_2 gene, encoding an iron acquisition protein [98]. Iron acquisition is

extremely important in intracellular bacterial survival and perhaps even more so in MAP. As little is known about mbth_2 and MAP iron metabolism in general at this time, more work is needed to fully understand what role this protein may plays in host cell death regulation and/or bacterial survival in macrophages.

The first major impact of this work is that future studies investigating cell death pathways, as well as other mechanisms, should consider bystander macrophages in MAP infected cultures. Previous work by our group and others studying MAP-macrophage interactions have studied a whole infected culture as a single unit. As demonstrated above, MAP-infected macrophages display a lower relative percentage of apoptotic cells than bystander macrophages. Therefore, use of whole culture based methods, such as RT-qPCR and western blotting, without accounting for potentially opposing features of infected and bystander cells, may yield results related to the *average* response of a population as opposed to the actual response of individual cells to infection. This would also be true of studies employing such techniques on infected tissues. Apoptosis gene expression results from our previous microarray work were inconclusive with regard to MAP infection either up-regulating or down-regulating apoptosis, likely a direct result of the bystander effect [73]. Pro-survival transcripts in MAP-infected macrophages were likely being mixed with pro-apoptotic transcripts in bystander macrophages and muting the true effects of MAP on infected cells. Consequently, precautions should be taken to monitor the relative percent of cells in a culture that are actually infected.

The second major impact of this research is the role that MAP-infection and apoptosis regulation play in treatment of the disease. Previously, we suggested that MAP-infection prevents apoptosis and efferocytosis as a way to circumvent the adaptive immune response. Based on this hypothesis, mycobacterial specific factors may play a very important role in the

altered regulation of host cell death, such as the role Rv3654c plays in MTB regulation of host cell apoptosis [89]. Future studies considering the role MAP prevention of host cell apoptosis plays in the whole immune system may better explain the spread of this disease in the host and the external environment.

Conclusion

Apoptosis of MAP-infected macrophages is important for the effective clearance of the bacterium from the host. However, our data demonstrates that MAP-infected macrophage populations contain a lower percentage of spontaneously apoptotic cells than uninfected cell populations in the same culture. Furthermore, these cells are much less likely to undergo apoptosis even after strong induction from agents such as H_2O_2. MAP-infected macrophages also show a drastically lower ability to activate caspases and contain lower caspase 3, 7 and 8 mRNA levels, which could be an explanation for the reduction in the ability of infected cells to enter apoptosis, relative to bystander macrophages and cells from uninfected control cultures. Future work focused on the bacteria driven host apoptotic regulation may result in new treatments and vaccine candidates for Johne's disease.

Acknowledgements

The authors would like to thank Dr. Melinda Wilson and Ms. Amber Dascelein Wilson for editorial assistance. We would also like to thank Dr. William Davis, Dr. Desmond Collins, and Dr. Adel Talaat for generously providing the mutant MAP strains for this project and Dr. Srinand Sreevatsen for providing MAP strain SS149. This work was supported through grants from the USDA-NIFA (2009-XXXXX) and the Johne's Disease Integrated Project, also through the USDA-NIFA (2011-85204-30025). Edward Kabara was supported through a USDA National Needs Graduate Fellowship grant (2007-XXXX).

Antibody	Company	Stock Number	Dilution
IgG1 Anti-FLIP	Enzo Life Sciences	ALX-804-428	1:25
IgG1 Anti-FADD	Abcam	AB10519	1:50
IgG1 Anti-BAD	Abcam	AB62480-100	1:50
IgG1 Anti-pAKT	Santa Cruz Biotechnology	SC-81433	1:25
IgG1 Anti-pBAD	Santa Cruz Biotechnology	SC-271963	1:25
IgG1 Anti-MCL-1	Abcam	AB31948	1:25
IgG1 Anti-ERK	Sigma-Aldrich	M3807	1:50
IgG1 Anti-pERK	Sigma-Aldrich	M8159	1:50
IgG1 Anti-pJNK	Sigma-Aldrich	J4750	1:50
IgG2A Anti-pp38	Sigma-Aldrich	M8177	1:50
IgG2A Anti-JNK	Sigma-Aldrich	SAB4200176	1:25
IgG2A Anti-TRADD	AbD Serotec	MCA4825Z	1:50
IgG2B Anti-p38	Sigma-Aldrich	M8432	1:25
IgG2B Anti-AKT	GenWay Bio	20-787-276352	1:25
Alexa Flour 488 Anti-IgG1	Invitrogen	A21121	1:1000
Alexa Flour 488 Anti-IgG2A	Invitrogen	A21131	1:1000
Alexa Flour 488 Anti-IgG2B	Invitrogen	M32501	1:200

TABLE 4.1 Antibodies Used in Flow Cytometry As part of the MAPK flow cytometry study, several different antibodies were used. For each antibody, the Company, Stock Number, and dilution are listed above.

Strain Number	Mutation	Mutated Gene
204	phage / site directed mutation	*lsr2*/ deletion (MAP0460)
213	Transposon mutagenesis (Tn5367)	MAP1566
214	ppiA gene (MAP0011)	MAP0011
218	Homologous recombination	MAP4287c
219	Transposon mutagenesis (Tn 5367)	MAP2408c
221	Homologous recombination	MAP1719c
222	Transposon mutagenesis (Tn 5367)	MAP1872c

TABLE 4.2 Mutant MAP Strains Several different mutant MAP strains were used in our study. For each mutant MAP strain used in our study, the nature of the mutation as well as the gene involved is shown.

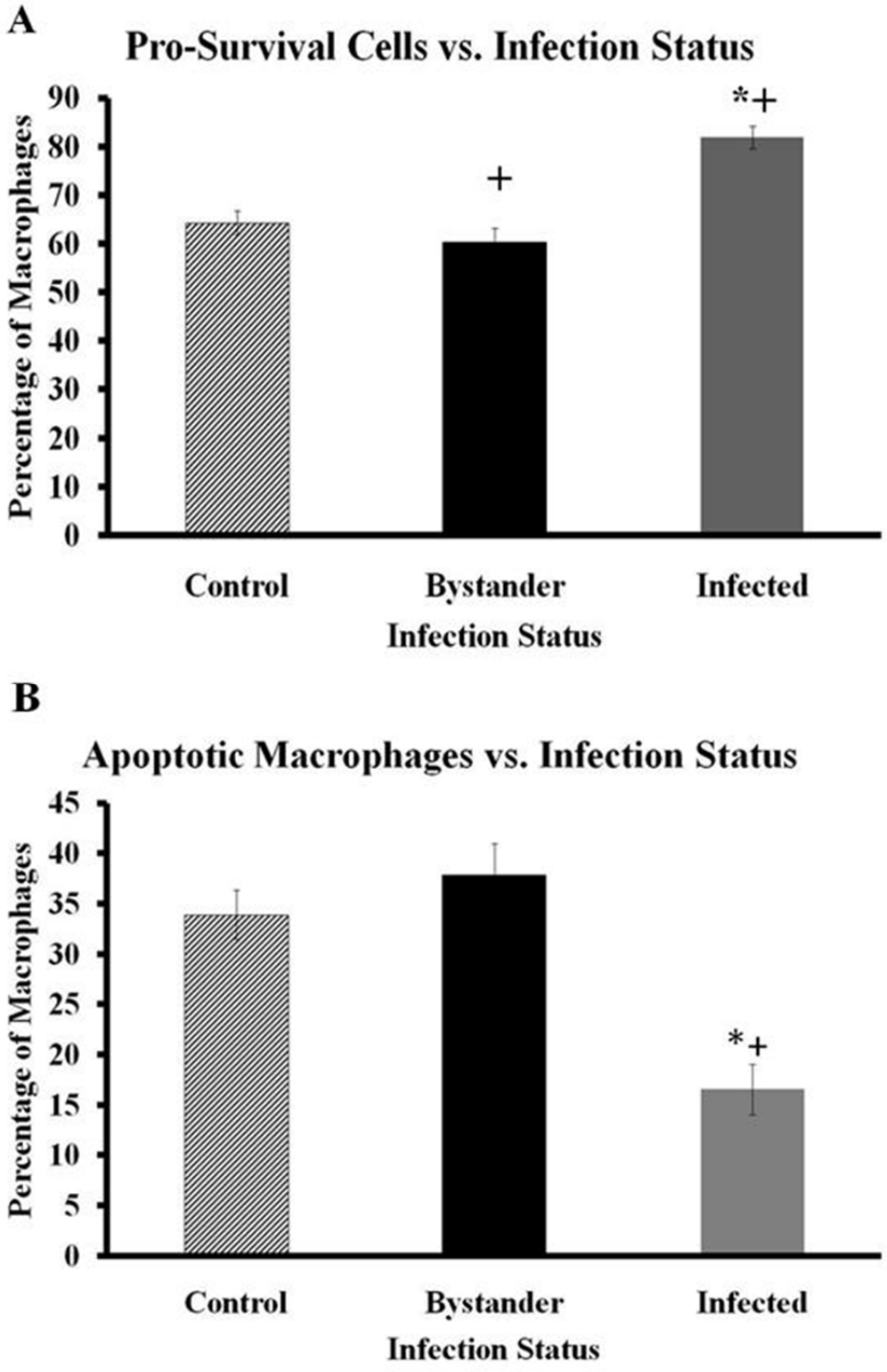

Figure 4.1-Apoptotic and pro-survival cells in populations of MAP-infected, bystander, and uninfected control cells. The percentage of apoptotic and pro-survival macrophages was

determined by flow cytometry as described in Materials and Methods. The bars represent the average results of MDM cultured from six individual healthy Holstein cattle. Error bars represent Standard Error of the mean (SEM) between the six biological replicates. + indicates significantly different from control, uninfected cells at $p < 0.05$ and * indicates significantly different from the bystander macrophage population at $p < 0.05$. Panel A depicts the percentage of MDM from the three cell populations that are apoptotic (Annexin V positive) while Panel B represents cells from each population that are pro-survival (Annexin V and 7-AAD negative).

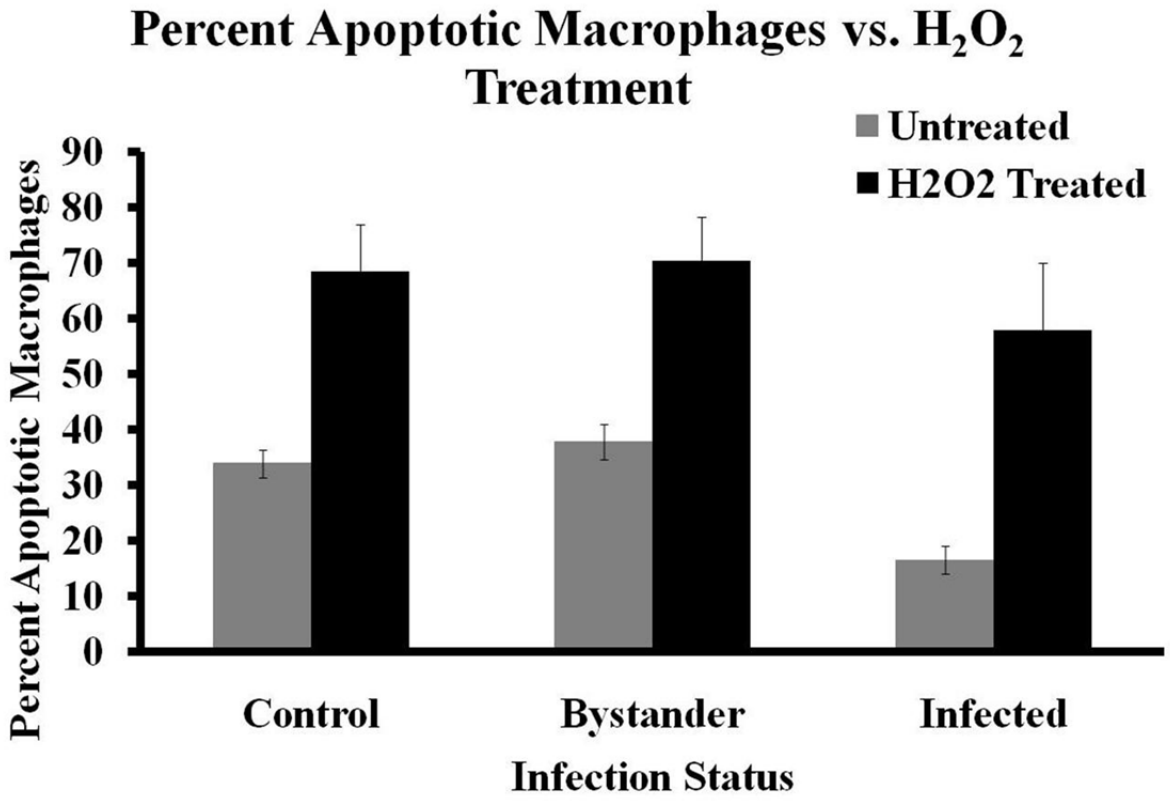

Figure 4.2-Cell status post apoptotic induction. Percentage of apoptotic macrophages in populations of MAP-infected, bystander and uninfected control cells was determined by flow cytometry after 20 minutes of 100uM H_2O_2 treatment. Bars represent the average results of MDM cultured from six healthy Holstein cattle. Grey bars represent the percentage of apoptotic

cells pre-treatment, while black bars represent the percentage of apoptotic macrophages after treatment in the three cell groups. Error bars represent Standard Error of the mean (SEM) between the six biological replicates. A + indicates significantly different from control, uninfected cells at $p < 0.05$ and * indicates significantly different from bystander macrophages at $p < 0.05$.

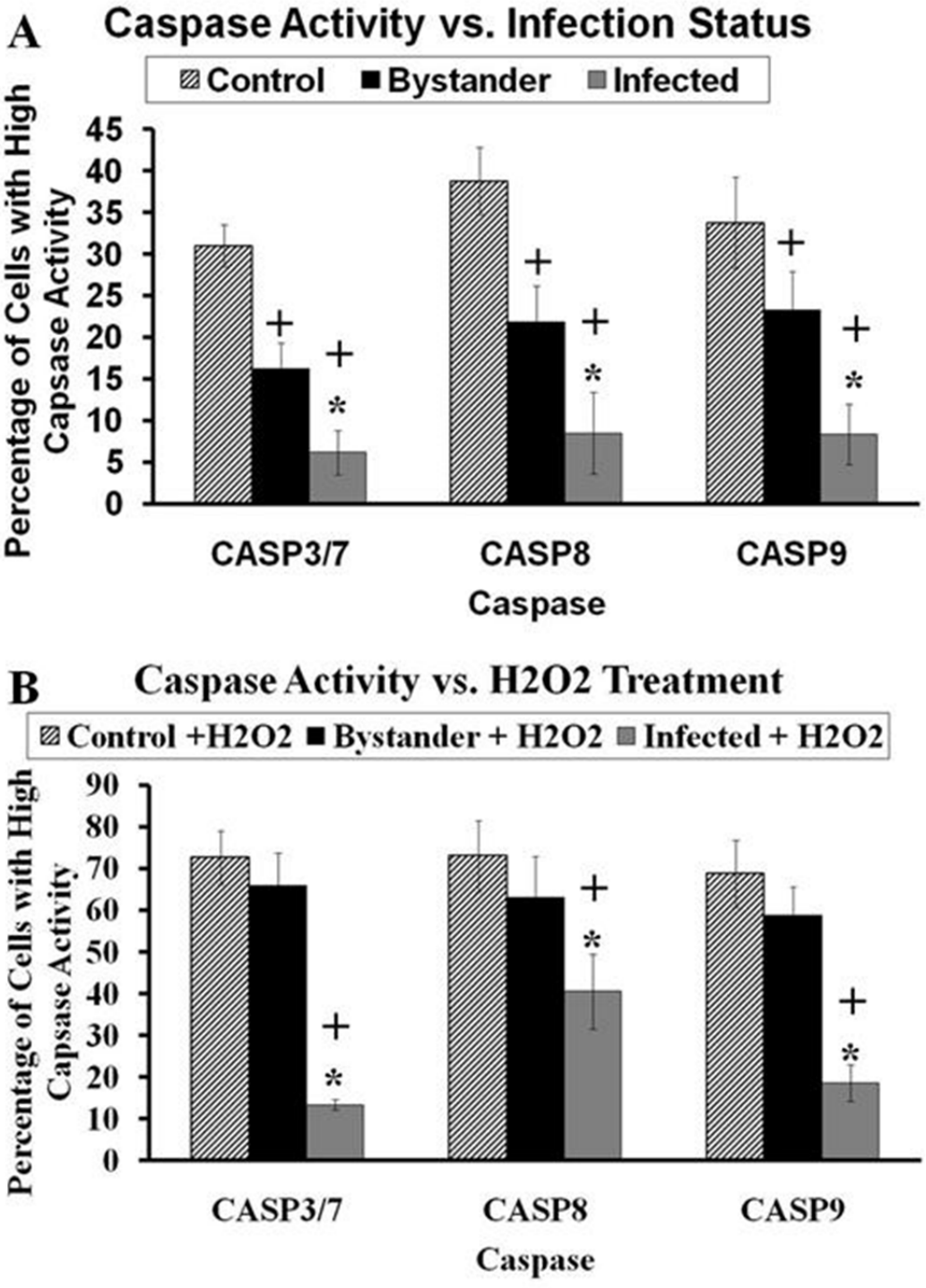

Figure 4.3- Caspase 3/7, 8, and 9 activity with and without H_2O_2 treatment. The percentage of cells with high activity for caspases 3/7, 8, and 9 in various cell populations was determined

using flow cytometry, as described in Materials and Methods. Bars represent the average results of MDM cultured from six healthy Holstein cattle. Error bars represent Standard error of the mean (SEM) between the six biological replicates. A + indicates significantly different from control, uninfected cell cultures at $p < 0.05$ and * indicates significantly different from bystander macrophage populations at $p < 0.05$. Data in Panel A represents the percentage of cells with high caspase activity without any apoptosis induction. Panel B shows the percentage of cells that display high caspase activity after 20 minutes of exposure to 100um H_2O_2.

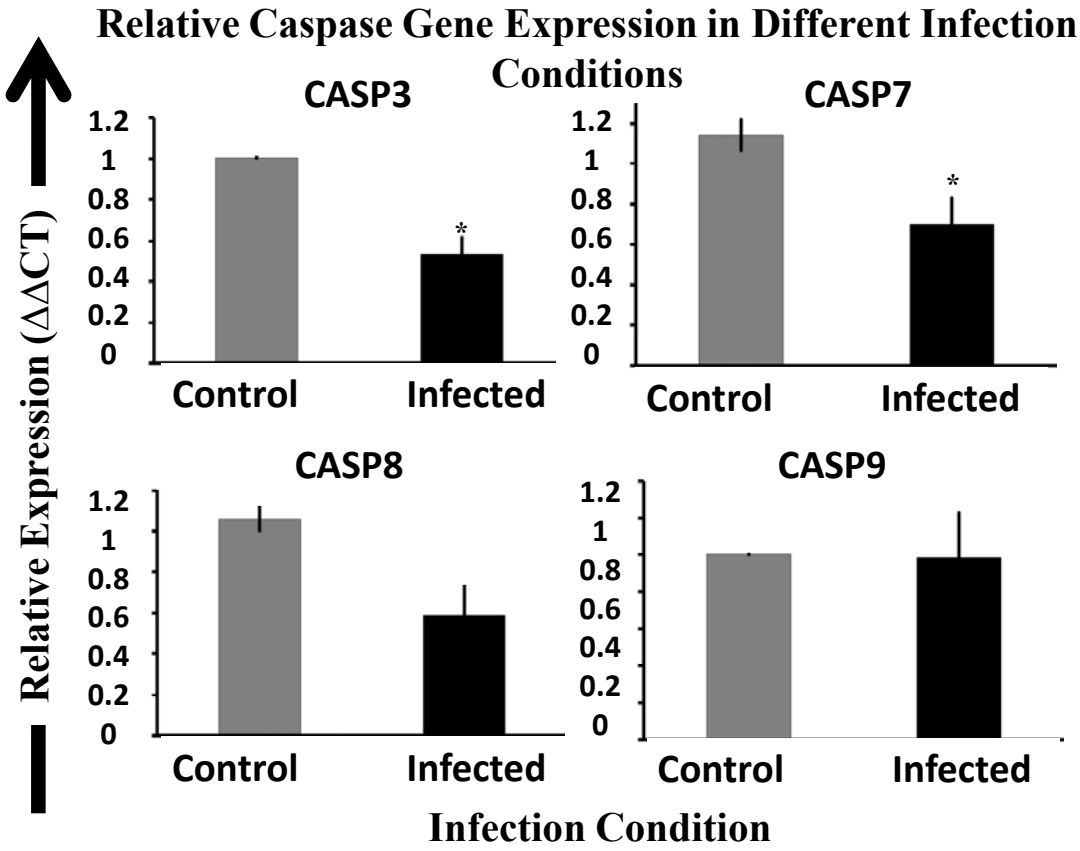

Figure 4.4-Relative expression of caspase genes in control and MAP-infected macrophages Abundance of mRNA encoding caspases 3, 7, 8, and 9 was determined via RT-qPCR as described in Materials and Methods. The ΔΔCt method was used to determine relative mRNA

abundance using beta-actin as the control gene. The uninfected sample (control) is indicated by grey boxes while infected samples are shown as black boxes. Bars represent the average results of MDM cultured from eight healthy Holstein cattle. Error bars represent standard error of the mean (SEM) between the eight biological replicates. Samples marked with a star (*) indicate samples that are significantly different then control samples at $p < 0.05$.

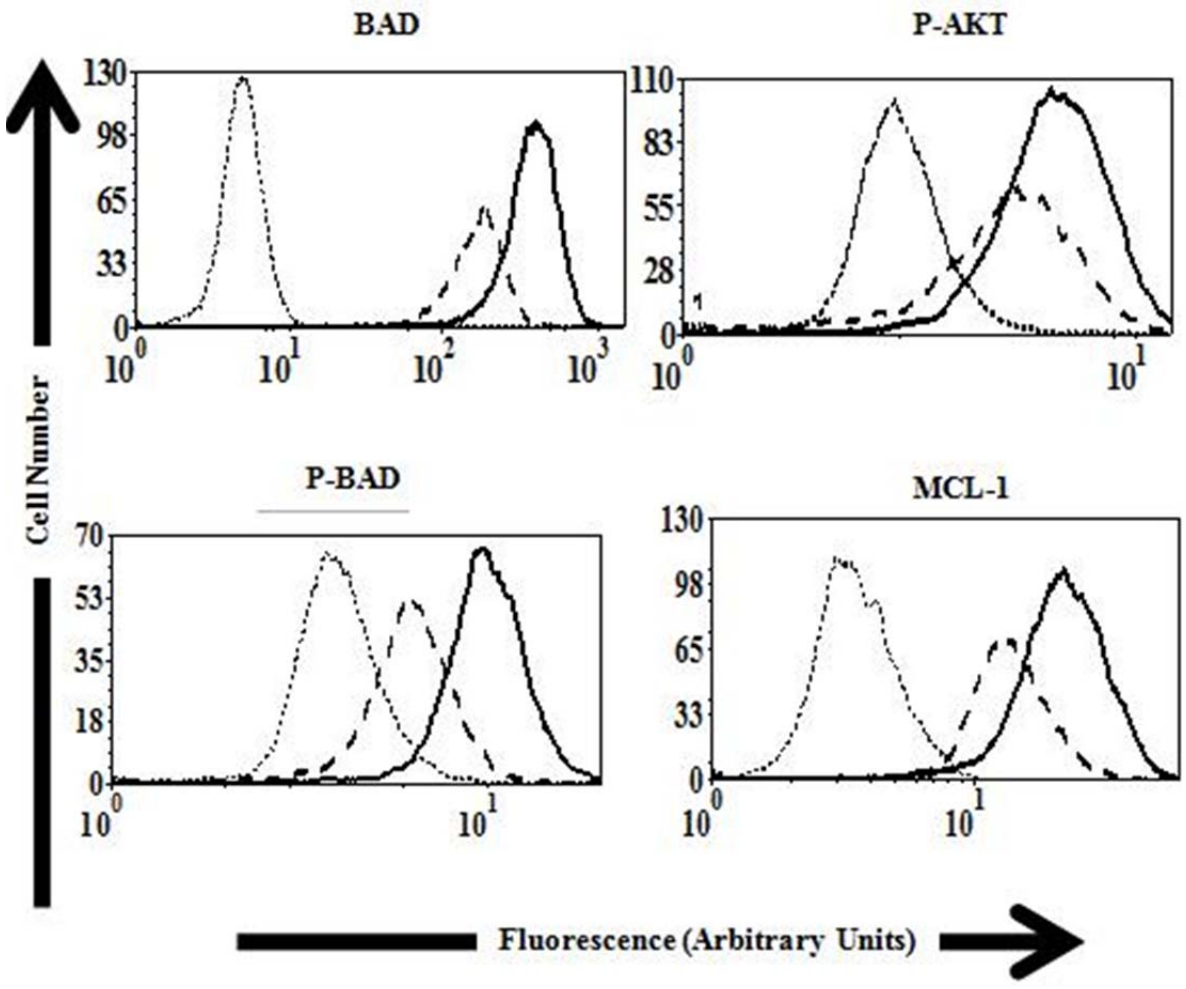

Figure 4.5-Protein expression in control and MAP-infected macrophages. Representative histograms used to determine relative protein expression via flow cytometry as described in Materials and Methods. The dotted line represents isotype control samples. The dashed line

represents data from MAP-infected macrophage populations. Solid black lines represent control, uninfected macrophage samples. Samples used to study p-AKT, BAD, and p-BAD were exposed to M-CSF prior to analysis. Samples used to study MCL-1 were exposed to GM-CSF prior to analysis.

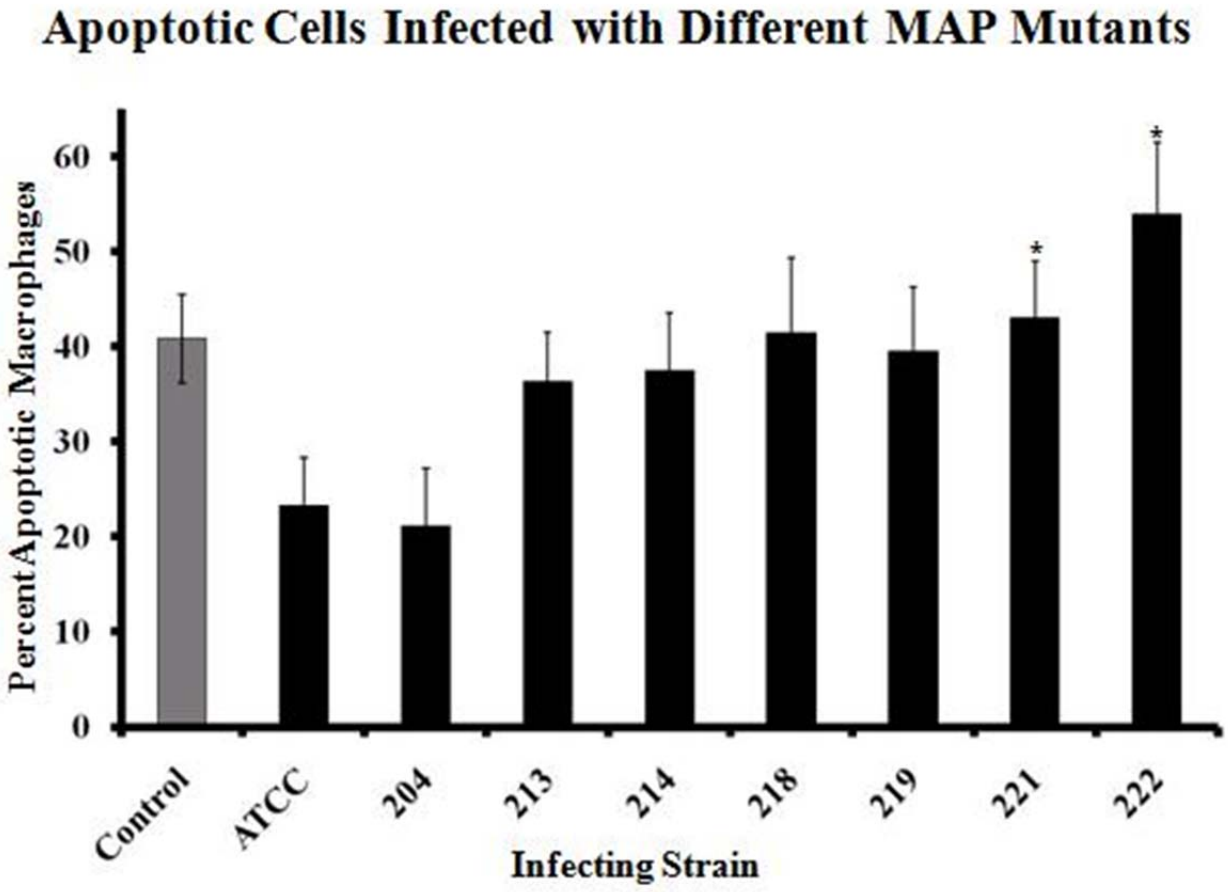

Figure 4.6- Macrophages infected with MAP mutants fail to prevent host cell apoptosis. The percentage of apoptotic macrophages was determined as described in Materials and Methods. Bars represent the average results of MDM cultured from four healthy Holstein cattle. Error bars represent standard error of the mean (SEM) between the four biological replicates. An * indicates significantly different from ATCC#19698 (ATCC)-infected macrophages at $p < 0.05$. The nature of each mutation is presented in Table 2, as described in the text.

Chapter 5

Summary and Future Considerations

My overarching goal with this project was to better understand the complex relationship between intracellular *Mycobacterium avium* subspecies *paratuberculosis* and bovine macrophages. The project started with a large-scale transcriptome analysis of macrophages cells experimentally infected with MAP. I found several host pathways and genes potentially involved in host-bacteria interactions. As part of my transcriptome study, I presented a way to reannotate the sequences on a microarray quickly and efficiently. Focusing the bacterial-macrophage studies to a single host pathway, we examined the interplay between MAP and infected macrophages in regulation of host cell apoptosis. We found that MAP-infection resulted in significant alteration of host macrophage apoptosis and apoptotic machinery. In addition, we proposed a generalized model for how MAP-infection may regulate host macrophage apoptosis in a manner beneficial to bacterial spread and survival in the host.

Initially, I conducted a large-scale gene expression study. By examining the transcriptomes of MAP-infected macrophages and uninfected macrophages, we showed that MAP-infection alters expression of a specific group of host genes. We found 92 transcripts that were commonly regulated in MAP-infection. Of these transcripts, 78 were found to have significant homology to sequences in the human genome, which we used as the basis of our analysis. Five of these sequences were completely new additions to the collection of genes related to mycobacterium-host interaction. To study such a large number of sequences in an effective way, the Database for Annotation, Visualization and Integrated Discovery (DAVID) was used to compare several databases. DAVID analysis showed that apoptosis regulation was significantly altered in MAP-infected macrophages when compared to control cells. Focusing on

genes involved in apoptotic signaling, we demonstrated that MAP-infected macrophages have significantly altered expression of caspase 1, caspase 4, Bad and PARP1relative to controls. Our gene expression data indicated that MAP-infection results in significant alteration in the control of host cell apoptosis genes. We also performed a comparison of the transcriptomes of MAP-infected macrophages from each separate strain to one another via clustering analysis. We found that K10, a strain often used as a standard strain for MAP biology and host interaction research, is remarkably different than the other strains studied by our group. Therefore, we advise other researchers to utilize another commonly used strain, ATCC#19698, as their primary research strain. Our work used MAP strains obtained from several different species. However, macrophage transcriptome profiles from macrophages infected with the MAP strains isolated from similar species displayed no significant clustering.

Our group, like many others, needed a quick, accurate, and cost-effective method of microarray annotation. As part of the microarray project, we described such a method and freely provided instructions and code that allows straightforward annotation of a cDNA microarray provided on the Center for Animal Functional Genomics website. Using these instructions and scripts, I was able to annotate an additional 25% of the BOTL5 microarray.

Based on the microarray annotations and analysis of the microarray project, we next studied cell death in MAP-infected and control, uninfected macrophages. Here, we demonstrated the bystander effect in MAP-infected cultures. Bystander macrophage populations, uninfected macrophages in an infected culture, displayed a trend to have a higher percentage of apoptotic cells than populations of control, uninfected or MAP-infected macrophages. We also demonstrated that MAP-infected macrophage populations exhibit a significantly lower percentage of apoptotic cells then either control, uninfected or bystander

macrophage populations. Similar survival results were observed after strong apoptotic induction. Our data indicated that MAP-infection significantly reduced an infected cells ability to undergo apoptosis. To explain reduced apoptosis rates, we studied caspase activation in MAP infection. We found that MAP-infection reduced not only the basal caspase activity, but also the macrophage caspase response to apoptotic stimuli. We hypothesized that MAP-infection established control of caspase activation as a mechanism for the regulation of host cell apoptosis. To further elucidate the mechanism in MAP-infection control of host cell death, we undertook two distinct approaches. First, using RT-qPCR based methods we found that MAP-infection reduces the relative gene expression of caspase 3, caspase 7, and caspase 8. However, MAP-infection did not affect the expression of caspase 9. Our caspase data suggested that while control of caspase gene expression in MAP-infection is important, other mechanisms must exist for complete control of host cell death. Second, we used flow cytometry to study host apoptotic protein expression. We observed significant differences in several host proteins: BAD, phospho-BAD, phospho-AKT, and MCL-1. Our protein data suggested that mitochondria may play an important role in regulation of MAP-infected macrophage apoptosis.

Our research significantly advanced what is known about the complex interaction between MAP and host macrophages. We emphasized the role MAP-infection plays in host cell apoptosis. Our group identified several bovine genes implicated in pathways altered by MAP-infection. Of these genes, a significant proportion was found to be important for host cell death regulation. Furthermore, we created a model for cell death and bacterial spread in MAP-infection. In addition, we presented evidence on the bystander effect in MAP infection. We now advise other groups to consider the bystander effect in whole culture research methods.

Results from these studies may not account for the complex interactions between infected and bystander cells.

While this may be completion of my graduate research, this is far from the conclusion of this work. Our work has elucidated the link between MAP-infection and apoptosis, but many questions remain unanswered. Based on my data, I hypothesize that MAP-infection causes a reduction in caspase 3, 7, and 8 mRNA abundance, which results in a reduction in caspase activation and ultimately apoptosis. To conclusively prove this link, one would need to prevent caspase mRNA reduction in MAP-infection. Also, while I establish an outline for MAP-infection driven control of host cell apoptosis, further refinement of this pathway is needed. I propose moving this research to a macrophage cell line like BoMac and validating MAP-infection regulation of host cell apoptosis. With a cell line that mimics apoptosis in MAP-infected primary macrophages, over-expression vectors and siRNA techniques could be more easily applied than in primary cells. First, I would suggest using inducible caspase over-expression vectors to test if caspase mRNA expression is responsible for the reduction in apoptosis in MAP-infection. Through external inducible caspase expression, the mechanism employed in MAP infection to regulate caspase mRNA abundance would be unable to prevent apoptosis. Therefore, apoptosis rates in MAP-infected and control macrophage populations should not be significantly different. This experiment would validate my hypothesis and direct future research experiments. Next, I would focus the next experiments to determine the exact interactions between the infecting MAP bacteria and the host to identify how caspase mRNA abundance is regulated. Here siRNA vectors could specifically down-regulate any suspected host proteins involved in caspase regulation leading to refinement in our understanding of how MAP-infection regulates host cell apoptosis.

In addition to the apoptosis work, the original microarray work also presented several other interesting pathways to consider. While I only focused on apoptosis in MAP-macrophage interactions, the microarray pointed to several unexplored pathways in this interaction. Any one of these areas could be developed into a full research project. Also, as reannotation paper demonstrated, using new annotations or analysis techniques to evaluate the data may uncover new trends that were previously unavailable. My analysis of the microarray data was limited to the available information at the present time. While my work studying this data lead me to one area of study, future researchers studying this same data would uncover different research foci.

REFERENCES

REFERENCES

1. ***Johne's Disease on U.S. Dairies, 1991–2007*, U.S.D.o. Agriculture, Editor. 2008.**

2. **Jones, R.L., *Review of the economic impact of Johne's disease in the United States*, in *Johne's Disease. Current Trends in Research, Diagnosis and Management.*, A.R.M.a.P.R. Wood, Editor. 1989, Commonw. Sci. Ind. Res. Organ: Melborn, Victoria, Australia. p. 46-50.**

3. **Clark, D.L., Jr., et al., *Detection of Mycobacterium avium subspecies paratuberculosis: comparing fecal culture versus serum enzyme-linked immunosorbent assay and direct fecal polymerase chain reaction.* J Dairy Sci, 2008. 91(7): p. 2620-7.**

4. **Whittington, R.J., et al., *Survival and dormancy of Mycobacterium avium subsp. paratuberculosis in the environment.* Appl Environ Microbiol, 2004. 70(5): p. 2989-3004.**

5. **Chamberlin, W.M. and S.A. Naser, *Integrating theories of the etiology of Crohn's disease. On the etiology of Crohn's disease: questioning the hypotheses.* Med Sci Monit, 2006. 12(2): p. RA27-33.**

6. **Eltholth, M.M., et al., *Contamination of food products with Mycobacterium avium paratuberculosis: a systematic review.* J Appl Microbiol, 2009. 107(4): p. 1061-71.**

7. **Clarke, C.J., *The pathology and pathogenesis of paratuberculosis in ruminants and other species.* J Comp Pathol, 1997. 116(3): p. 217-61.**

8. **Coussens, P.M., *Mycobacterium paratuberculosis and the bovine immune system.* Anim Health Res Rev, 2001. 2(2): p. 141-61.**

9. **Chiang, S.K., et al., *Relationship between Mycobacterium avium subspecies paratuberculosis, IL-1alpha, and TRAF1 in primary bovine monocyte-derived macrophages.* Vet Immunol Immunopathol, 2007. 116(3-4): p. 131-44.**

10. **Sohal, J.S., et al., *Immunology of mycobacterial infections: with special reference to Mycobacterium avium subspecies paratuberculosis.* Immunobiology, 2008. 213(7): p. 585-98.**

11. **Desjardins, M., *Biogenesis of phagolysosomes: the 'kiss and run' hypothesis.* Trends Cell Biol, 1995. 5(5): p. 183-6.**

12. **Kuehnel, M.P., et al., *Characterization of the intracellular survival of Mycobacterium avium ssp. paratuberculosis: phagosomal pH and fusogenicity in J774 macrophages compared with other mycobacteria.* Cell Microbiol, 2001. 3(8): p. 551-66.**

13. **Spickler, A.R., *Paratuberculosis (Johne's Disease) and Crohn's Disease*. 2006.**

14. **Tanaka, S., et al., *Inflammatory cytokine gene expression in different types of granulomatous lesions during asymptomatic stages of bovine paratuberculosis.* Vet Pathol, 2005. 42(5): p. 579-88.**

15. **Rowe, M.T. and I.R. Grant, *Mycobacterium avium ssp. paratuberculosis and its potential survival tactics.* Lett Appl Microbiol, 2006. 42(4): p. 305-11.**

16. **Johne, H.A., and J. Frothingham., *Ein eigenthuemlicher fall von tuberculose beim rind.* Dtsch. Z. Tiermed. Pathol., 1985. 21: p. 438-454.**

17. **Begg, D.J. and J.F. Griffin, *Vaccination of sheep against M. paratuberculosis: immune parameters and protective efficacy.* Vaccine, 2005. 23(42): p. 4999-5008.**

18. **McDonald, W.L., et al., *Evaluation of diagnostic tests for Johne's disease in young cattle.* Aust Vet J, 1999. 77(2): p. 113-9.**

19. **Ellingson, J.L., et al., *Detection of viable Mycobacterium avium subsp. paratuberculosis in retail pasteurized whole milk by two culture methods and PCR.* J Food Prot, 2005. 68(5): p. 966-72.**

20. **Clark, D.L., Jr., et al., *Detection of Mycobacterium avium subspecies paratuberculosis genetic components in retail cheese curds purchased in Wisconsin and Minnesota by PCR.* Mol Cell Probes, 2006. 20(3-4): p. 197-202.**

21. **El-Zaatari, F.A., M.S. Osato, and D.Y. Graham, *Etiology of Crohn's disease: the role of Mycobacterium avium paratuberculosis.* Trends Mol Med, 2001. 7(6): p. 247-52.**

22. **Nguyen, L. and J. Pieters, *The Trojan horse: survival tactics of pathogenic mycobacteria in macrophages.* Trends Cell Biol, 2005. 15(5): p. 269-76.**

23. ***Tuberculosis*. Fact sheets 2007 March 2007 [cited 2007 August 1, 2007]; Available from: http://www.who.int/mediacentre/factsheets/fs104/en/index.html.**

24. **Hashimoto, T., *[Experimental studies on the mechanism of infection and immunity in tuberculosis from the analytical standpoint of streptomycin-dependent tubercle bacilli. 1. Isolation and biological characteristics of a streptomycin-dependent mutant, and effect of streptomycin administration on its pathogenicity in guinea-pigs.].* Kekkaku, 1955. 30(1): p. 4-8; English summary, 45-6.**

25. **Coussens, P.M., *Model for immune responses to Mycobacterium avium subspecies paratuberculosis in cattle.* Infect Immun, 2004. 72(6): p. 3089-96.**

26. **Murphy, J.T., et al., *Gene expression profiling of monocyte-derived macrophages following infection with Mycobacterium avium subspecies avium and Mycobacterium avium subspecies paratuberculosis.* Physiol Genomics, 2006. 28(1): p. 67-75.**

27. **Janagama, H.K., et al., *Cytokine responses of bovine macrophages to diverse clinical Mycobacterium avium subspecies paratuberculosis strains.* BMC Microbiol, 2006. 6(1): p. 10.**

28. **Woo, S.R., et al., *Bovine monocytes and a macrophage cell line differ in their ability to phagocytose and support the intracellular survival of Mycobacterium avium subsp. paratuberculosis.* Vet Immunol Immunopathol, 2006. 110(1-2): p. 109-20.**

29. **Churchill, G.A., *Fundamentals of experimental design for cDNA microarrays.* Nat Genet, 2002. 32 Suppl: p. 490-5.**

30. **Allison, D.B., et al., *A mixture model approach for the analysis of microarray gene expression data.* Computational Statistics & Data Analysis, 2002. 39(1): p. 1-20.**

31. **Eisen, M.B., et al., *Cluster analysis and display of genome-wide expression patterns.* Proc Natl Acad Sci U S A, 1998. 95(25): p. 14863-8.**

32. **Dennis, G., Jr., et al., *DAVID: Database for Annotation, Visualization, and Integrated Discovery.* Genome Biol, 2003. 4(5): p. P3.**

33. **Coussens, P.M., et al., *Johne's disease in cattle is associated with enhanced expression of genes encoding IL-5, GATA-3, tissue inhibitors of matrix metalloproteinases 1 and 2, and factors promoting apoptosis in peripheral blood mononuclear cells.* Vet Immunol Immunopathol, 2005. 105(3-4): p. 221-34.**

34. **Coussens, P.M., et al., *Cytokine gene expression in peripheral blood mononuclear cells and tissues of cattle infected with Mycobacterium avium subsp. paratuberculosis: evidence for an inherent proinflammatory gene expression pattern.* Infect Immun, 2004. 72(3): p. 1409-22.**

35. **Coussens, P.M., et al., *Gene expression profiling of peripheral blood mononuclear cells from cattle infected with Mycobacterium paratuberculosis.* Infect Immun, 2002. 70(10): p. 5494-502.**

36. **Marsh, I.B., et al., *Genomic comparison of Mycobacterium avium subsp. paratuberculosis sheep and cattle strains by microarray hybridization.* J Bacteriol, 2006. 188(6): p. 2290-3.**

37. **Kelly, D.M., et al., *Bystander macrophage apoptosis after Mycobacterium tuberculosis H37Ra infection.* Infect Immun, 2008. 76(1): p. 351-60.**

38. **Collins, D.M., D.M. Gabric, and G.W. de Lisle, *Identification of two groups of Mycobacterium paratuberculosis strains by restriction endonuclease analysis and DNA hybridization.* J Clin Microbiol, 1990. 28(7): p. 1591-6.**

39. **de Lisle, G.W., G.F. Yates, and D.M. Collins, *Paratuberculosis in farmed deer: case reports and DNA characterization of isolates of Mycobacterium paratuberculosis.* J Vet Diagn Invest, 1993. 5(4): p. 567-71.**

40. **Whittington, R.J., et al., *Molecular epidemiology of Mycobacterium avium subsp. paratuberculosis: IS900 restriction fragment length polymorphism and IS1311 polymorphism analyses of isolates from animals and a human in Australia.* J Clin Microbiol, 2000. 38(9): p. 3240-8.**

41. **Motiwala, A.S., et al., *Molecular epidemiology of Mycobacterium avium subsp. paratuberculosis isolates recovered from wild animal species.* J Clin Microbiol, 2004. 42(4): p. 1703-12.**

42. **Wu, C.W., et al., *Optical mapping of the Mycobacterium avium subspecies paratuberculosis genome.* BMC Genomics, 2009. 10: p. 25.**

43. **Weiss, D.J., et al., *Gene expression and antimicrobial activity of bovine macrophages in response to Mycobacterium avium subsp. paratuberculosis.* Vet Pathol, 2004. 41(4): p. 326-37.**

44. **Winau, F., S.H. Kaufmann, and U.E. Schaible, *Apoptosis paves the detour path for CD8 T cell activation against intracellular bacteria.* Cell Microbiol, 2004. 6(7): p. 599-607.**

45. **Keane, J., H.G. Remold, and H. Kornfeld, *Virulent Mycobacterium tuberculosis strains evade apoptosis of infected alveolar macrophages.* J Immunol, 2000. 164(4): p. 2016-20.**

46. **Liu, X., et al., *DFF, a heterodimeric protein that functions downstream of caspase-3 to trigger DNA fragmentation during apoptosis.* Cell, 1997. 89(2): p. 175-84.**

47. **Nicholson, D.W., et al., *Identification and inhibition of the ICE/CED-3 protease necessary for mammalian apoptosis.* Nature, 1995. 376(6535): p. 37-43.**

48. **Faucheu, C., et al., *A novel human protease similar to the interleukin-1 beta converting enzyme induces apoptosis in transfected cells.* Embo J, 1995. 14(9): p. 1914-22.**

49. **Keller, M., et al., *Active caspase-1 is a regulator of unconventional protein secretion.* Cell, 2008. 132(5): p. 818-31.**

50. **Barnes, P.J. and M. Karin, *Nuclear factor-kappaB: a pivotal transcription factor in chronic inflammatory diseases.* N Engl J Med, 1997. 336(15): p. 1066-71.**

51. **Dong, W., et al., *The IRAK-1-BCL10-MALT1-TRAF6-TAK1 cascade mediates signaling to NF-kappaB from Toll-like receptor 4.* J Biol Chem, 2006. 281(36): p. 26029-40.**

52. **Lee, J.S., et al., *Expression and regulation of the CC-chemokine ligand 20 during human tuberculosis.* Scand J Immunol, 2008. 67(1): p. 77-85.**

53. **Ray, J.C., J.L. Flynn, and D.E. Kirschner, *Synergy between individual TNF-dependent functions determines granuloma performance for controlling Mycobacterium tuberculosis infection.* J Immunol, 2009. 182(6): p. 3706-17.**

54. **Lemke, G. and Q. Lu, *Macrophage regulation by Tyro 3 family receptors.* Curr Opin Immunol, 2003. 15(1): p. 31-6.**

55. **Lettre, G. and J.D. Rioux, *Autoimmune diseases: insights from genome-wide association studies.* Hum Mol Genet, 2008. 17(R2): p. R116-21.**

56. **Waddell, L.A., et al., *The zoonotic potential of Mycobacterium avium spp. paratuberculosis: a systematic review.* Can J Public Health, 2008. 99(2): p. 145-55.**

57. **Quante, M., et al., *No functional and transductional significance of specific neuropilin 1 siRNA inhibition in colon carcinoma cell lines lacking VEGF receptor 2.* Oncol Rep, 2009. 21(5): p. 1161-8.**

58. **Byrd, V.M., et al., *Fibroblast growth factor-1 (FGF-1) enhances IL-2 production and nuclear translocation of NF-kappaB in FGF receptor-bearing Jurkat T cells.* J Immunol, 1999. 162(10): p. 5853-9.**

59. **Korf, H., et al., *Liver X receptors contribute to the protective immune response against Mycobacterium tuberculosis in mice.* J Clin Invest, 2009.**

60. **Chawla, A., et al., *Nuclear receptors and lipid physiology: opening the X-files.* Science, 2001. 294(5548): p. 1866-70.**

61. **Nuckels, R.J., et al., *The vacuolar-ATPase complex regulates retinoblast proliferation and survival, photoreceptor morphogenesis, and pigmentation in the zebrafish eye.* Invest Ophthalmol Vis Sci, 2009. 50(2): p. 893-905.**

62. **Cheville, N.F., et al., *Intracellular trafficking of Mycobacterium avium ss. paratuberculosis in macrophages.* Dtsch Tierarztl Wochenschr, 2001. 108(6): p. 236-43.**

63. ***Online Mendelian Inheritance in Man, OMIM (TM).* 2009 [cited; Available from: http://www.ncbi.nlm.nih.gov/omim/**

64. **Glatzel, A., et al., *Patterns of chemokine receptor expression on peripheral blood gamma delta T lymphocytes: strong expression of CCR5 is a selective feature of V delta 2/V gamma 9 gamma delta T cells.* J Immunol, 2002. 168(10): p. 4920-9.**

65. **Bermudez, L.E., A. Parker, and M. Petrofsky, *Apoptosis of Mycobacterium avium-infected macrophages is mediated by both tumour necrosis factor (TNF) and Fas, and involves the activation of caspases.* Clin Exp Immunol, 1999. 116(1): p. 94-9.**

66. **Wieland, C.W., et al., *Pulmonary Mycobacterium tuberculosis infection in leptin-deficient ob/ob mice.* Int Immunol, 2005. 17(11): p. 1399-408.**

67. **Werninghaus, K., et al., *Adjuvanticity of a synthetic cord factor analogue for subunit Mycobacterium tuberculosis vaccination requires FcRgamma-Syk-Card9-dependent innate immune activation.* J Exp Med, 2009. 206(1): p. 89-97.**

68. **Marchal, G., *[Preferential differentiation of hematopoietic stem cells in mice after intravenous injection of BCG].* C R Acad Sci Hebd Seances Acad Sci D, 1976. 282(20): p. 1829-32.**

69. **Camacho, C., et al., *BLAST+: architecture and applications.* BMC Bioinformatics, 2009. 10(421): p. 421.**

70. **Altschul, S.F., et al., *Basic local alignment search tool.* J Mol Biol, 1990. 215(3): p. 403-10.**

71. **Yao, J., et al., *Generation of EST and cDNA microarray resources for the study of bovine immunobiology.* Acta Vet Scand, 2001. 42(3): p. 391-405.**

72. **Hostetter, J., et al., *Phagosomal maturation and intracellular survival of Mycobacterium avium subspecies paratuberculosis in J774 cells.* Comp Immunol Microbiol Infect Dis, 2003. 26(4): p. 269-83.**

73. **Kabara, E., et al., *A large-scale study of differential gene expression in monocyte-derived macrophages infected with several strains of Mycobacterium avium subspecies paratuberculosis.* Brief Funct Genomics. 9(3): p. 220-37.**

74. **Abramovitch, R.B. and G.B. Martin, *Strategies used by bacterial pathogens to suppress plant defenses.* Curr Opin Plant Biol, 2004. 7(4): p. 356-64.**

75. **Stuart, L.M. and R.A. Ezekowitz, *Phagocytosis: elegant complexity.* Immunity, 2005. 22(5): p. 539-50.**

76. **Mares, C.A., et al., *Defect in efferocytosis leads to alternative activation of macrophages in Francisella infections.* Immunol Cell Biol. 89(2): p. 167-72.**

77. **Roppenser, B., et al., *Yersinia enterocolitica differentially modulates RhoG activity in host cells.* J Cell Sci, 2009. 122(Pt 5): p. 696-705.**

78. **Thorp, E., et al., *Mertk receptor mutation reduces efferocytosis efficiency and promotes apoptotic cell accumulation and plaque necrosis in atherosclerotic lesions of apoe-/- mice.* Arterioscler Thromb Vasc Biol, 2008. 28(8): p. 1421-8.**

79. **Sly, L.M., et al., *Survival of Mycobacterium tuberculosis in host macrophages involves resistance to apoptosis dependent upon induction of antiapoptotic Bcl-2 family member Mcl-1.* J Immunol, 2003. 170(1): p. 430-7.**

80. **Fratazzi, C., et al., *Programmed cell death of Mycobacterium avium serovar 4-infected human macrophages prevents the mycobacteria from spreading and induces mycobacterial growth inhibition by freshly added, uninfected macrophages.* J Immunol, 1997. 158(9): p. 4320-7.**

81. **Lee, J., M. Hartman, and H. Kornfeld, *Macrophage apoptosis in tuberculosis.* Yonsei Med J, 2009. 50(1): p. 1-11.**

82. **Rojas, M., et al., *Differential induction of apoptosis by virulent Mycobacterium tuberculosis in resistant and susceptible murine macrophages: role of nitric oxide and mycobacterial products.* J Immunol, 1997. 159(3): p. 1352-61.**

83. **Danelishvili, L., et al., *Mycobacterium tuberculosis infection causes different levels of apoptosis and necrosis in human macrophages and alveolar epithelial cells.* Cell Microbiol, 2003. 5(9): p. 649-60.**

84. **Chattree, V., et al., *Inhibition of apoptosis, activation of NKT cell and upregulation of CD40 and CD40L mediated by M. leprae antigen(s) combined with Murabutide and Trat peptide in leprosy patients.* Mol Cell Biochem, 2008. 309(1-2): p. 87-97.**

85. **Ryter, S.W., et al., *Mechanisms of cell death in oxidative stress.* Antioxid Redox Signal, 2007. 9(1): p. 49-89.**

86. **Maiti, D., A. Bhattacharyya, and J. Basu, *Lipoarabinomannan from Mycobacterium tuberculosis promotes macrophage survival by phosphorylating Bad through a phosphatidylinositol 3-kinase/Akt pathway.* J Biol Chem, 2001. 276(1): p. 329-33.**

87. **Hasan, Z., et al., *M. leprae inhibits apoptosis in THP-1 cells by downregulation of Bad and Bak and upregulation of Mcl-1 gene expression.* BMC Microbiol, 2006. 6(78): p. 78.**

88. **Pena, A.S., O. Karimi, and J.B. Crusius, *A new avenue to investigate: the autophagic process. From Crohn's disease to Chlamydia.* Drugs Today (Barc), 2009. 45 Suppl B: p. 113-7.**

89. **Danelishvili, L., et al., *Secreted Mycobacterium tuberculosis Rv3654c and Rv3655c proteins participate in the suppression of macrophage apoptosis.* PLoS One. 5(5): p. e10474.**

90. **Danial, N.N., *BAD: undertaker by night, candyman by day.* Oncogene, 2008. 27 Suppl 1(1): p. S53-70.**

91. **Thomas, L.W., C. Lam, and S.W. Edwards, *Mcl-1; the molecular regulation of protein function.* FEBS Lett. 584(14): p. 2981-9.**

92. **Cadieux, N., et al., *Induction of cell death after localization to the host cell mitochondria by the Mycobacterium tuberculosis PE_PGRS33 protein.* Microbiology. 157(Pt 3): p. 793-804.**

93. **Duan, L., et al., *Critical role of mitochondrial damage in determining outcome of macrophage infection with Mycobacterium tuberculosis.* J Immunol, 2002. 169(9): p. 5181-7.**

94. **Gan, H., et al., *Enhancement of antimycobacterial activity of macrophages by stabilization of inner mitochondrial membrane potential.* J Infect Dis, 2005. 191(8): p. 1292-300.**

95. **Sommer, S., et al., *Mycobacterium avium subspecies paratuberculosis suppresses expression of IL-12p40 and iNOS genes induced by signalling through CD40 in bovine monocyte-derived macrophages.* Vet Immunol Immunopathol, 2009. 128(1-3): p. 44-52.**

96. **Av-Gay, Y. and M. Everett, *The eukaryotic-like Ser/Thr protein kinases of Mycobacterium tuberculosis.* Trends Microbiol, 2000. 8(5): p. 238-44.**

97. **Vergne, I., et al., *Cell biology of mycobacterium tuberculosis phagosome.* Annu Rev Cell Dev Biol, 2004. 20: p. 367-94.**

98. **Zhu, X., et al., *Transcriptional analysis of diverse strains Mycobacterium avium subspecies paratuberculosis in primary bovine monocyte derived macrophages.* Microbes Infect, 2008. 10(12-13): p. 1274-82.**